Relative Stabilities of Weakly Coordinating Anions: A Computational Study

Ingo Krossing* and Ines Raabe[a]

Abstract: This article describes BP86/SV(P) (DFT) calculations on a representative set of weakly coordinating anions (WCAs) of type $[M(L)_n]^-$, their parent neutral Lewis acids $M(L)_{n-1}$ and their ate complexes with fluoride, that is, $[FM(L)_n]^{n-1}$ (M = B, L = F, $OTeF_5$, C_6H_5, C_6F_5, $C_6H_3(CF_3)_2$, CF_3; M = P, As, Sb, L = F, $OTeF_5$; M = Al, L = $OC(CF_3)_3$). Compounds with fluoride bridges, that is, Sb_nF_{5n} and $[Sb_nF_{5n+1}]^-$ (n = 2, 3, 4), $Al_2(L)_5F$ and $[(L)_3Al\text{-}F\text{-}Al(L)_3]^-$ (L = $OC(CF_3)_3$), $(F_4C_6\{1,2\text{-}B(L)_2\}_2$, $[F_4C_6\{1,2\text{-}B(L)_2\}_2F]^-$, $[F_4C_6\{1,2\text{-}B(L)_2\}_2OMe]^-$ (L = C_6F_5) were also calculated. Based on these BP86/SV(P) and auxiliary MP2/TZVPP, G2, and CBS-Q calculations the relative stabilities and coordinating abilities of these WCAs were established with regard to the fluoride ion affinities (FIA) of the parent Lewis acids, the ligand affinity (LA) of the WCAs, the decomposition of a given WCA in the presence of a hard (H^+, proton decomposition PD) and a soft electrophile (Cu^+, copper decomposition CuD), the position of the HOMO, the HOMO–LUMO gap, and population analyses of the anions providing partial charges for all atoms. To obtain data that is more reliable, the assessed quantities were calculated through isodesmic reactions. If parts of the calculations could not be done isodesmically, higher levels such as MP2/TZVPP, G2, and CBS-Q were used to obtain reliable values for these reactions. Although the obtained results can not be taken as absolute, the relative ordering of the stabilities of all WCAs will undoubtedly be correct, since a single methodology was chosen for the investigation. To include media effects the decomposition reactions of a subset of 14 WCAs with the $SiMe_3^+$ and $[Cp_2ZrMe]^+$ ions were also calculated in PhCl and 1,2-$F_2C_6H_4$ (COSMO solvation model). We found that in most cases gas-phase calculations and solution calculations give comparable results for the stability of the anion. Applications of the LA and FIA that allow one to decide, on thermodynamic grounds, which WCA or Lewis acid is the most suitable for a given problem are sketched.

Keywords: anions · density functional calculations · Lewis acids · solvent effects · thermodynamics

Introduction

Weakly coordinating anions (WCAs) are of great current interest and have impact on applied and fundamental science.[1,2] Applications of WCAs lie, for example, in homogenous catalysis,[3–5] polymerization chemistry,[1c,6,7] ionic liquids,[8,9] electrochemistry,[10–12] photolithography,[13–16] and lithium ion batteries.[17–19] More fundamental applications are the stabilization of reactive electrophilic cations or weakly bound adducts, for example, $AuXe_4^{2+}$,[20] Xe_2^+,[21] HC_{60}^+,[22] Mes_3Si^+,[23] $Ag(CO)_2^+$,[24] N_5^+,[25] $[Ir(CO)_6]^{3+}$,[26] $Ag(L)_2^+$ (L = P_4,[27] S_8,[28] P_4S_3[29]), $Ag(C_2H_4)_3^+$,[30] $P_5X_2^+$ (X = Br, I),[31] and CX_3^+ (X = Cl, Br, I).[32,33] Consequently, a large number of WCAs was developed in the last decade and recently reviewed in reference [1d].

One question that is still open is the reliable ordering of the relative stabilities and coordinating abilities of all types of WCAs known today. Earlier attempts used the ^{29}Si NMR shift of the $Si(iPr)_3^{\delta+}X^{\delta-}$ silylium ion pair (X = WCA) as a measure, whereby shifts to lower field indicate a more pronounced cationic character of the $Si(iPr)_3^{\delta+}$ part, which is an indication for a more weakly coordinating anion X^-.[34] However, inertness and coordinating ability of WCAs do not always come hand in hand, and therefore the reactive nature of the $Si(iPr)_3^{\delta+}$ part precludes the investigation of many anions that proved to be very weakly coordinating due to anion decomposition (e.g., all fluorometallates and teflate-based anions). A recent conference report by Reed evaluates the N–H stretching vibration of a series of ammonium salts $(n\text{-oct})_3NH^+[X]^-$ (X = WCA) in CCl_4 on the basis of the following assumption: The higher the frequency of

---

[a] Priv. Doz. Dr. I. Krossing, Dipl. Chem. I. Raabe
Universität Karlsruhe, Institut für Anorganische Chemie
Engesserstr. Geb. 30.45, 76128 Karlsruhe
Fax: +(49) 721-608-48-54
E-mail: krossing@chemie.uni-karlsruhe.de

Supporting information for this article is available on the WWW under http://www.chemeurj.org/ or from the author: Drawings of each calculated compound shown in Figure 1 and their parent Lewis acids and fluoride complexes, their basic structural parameters, and an *xyz* orientation (in Bohr units). Solvation energies of the calculated anions and their parent Lewis acids; total energies for Equations (12)–(18).

the stretching vibration, the less the anion interacts with the cation and the more weakly coordinating is $[X]^-$.[35] This scale gives an ordering of the relative coordinating ability of the WCA towards $(n\text{-oct})_3NH^+$ in CCl_4, but still awaits full publication.[35] To investigate the stabilities of fluorometalate anions such as BF_4^-, MF_6^- (M = P, As, Sb, etc.), the fluoride ion affinities (FIAs) of their parent Lewis acids A, that is, BF_3, MF_5, and so forth, were estimated on thermodynamic grounds [Eq. (1)]:[36]

$$A_{(g)} + F^-_{(g)} \xrightarrow{\Delta H=-\text{FIA}} AF^-_{(g)} \qquad (1)$$

The higher the FIA of the parent Lewis acid A of a given WCA, the more stable it is towards decomposition on thermodynamic grounds. Christe and Dixon chose a computational approach to obtain a larger relative Lewis acidity scale based on the calculation of the FIA in an isodesmic reaction with OCF_3^- and the experimental FIA of OCF_2 of 209 kJ mol^{-1}.[37] Others used the same methodology.[38–41] Hitherto, this approach was limited to relatively small systems.

In this contribution, we chose an entirely computational approach to allow comparison of the properties of very different types of WCAs such as the fluoroantimonates and perfluoroarylborates. The structures of WCAs of type $[M(L)_n]^-$ (L = monoanionic ligand), their parent Lewis acids $A = M(L)_{n-1}$, and the $AF^- = [FM(L)_{n-1}]^-$ ions were optimized with DFT methods at the (RI-)BP86/SV(P) level. With these calculated data and auxiliary (RI-)MP2/TZVPP, G2, and CBS-Q calculations, the thermodynamic stability and coordinating ability of the WCAs was established on the basis of the ligand affinity LA of the parent Lewis acid $A = M(L)_{n-1}$, the FIA of the parent Lewis acid A, as calculated with the methodology of Christe and Dixon,[37] the decomposition of a given anion in the presence of a hard (H^+, proton decomposition PD) and a soft electrophile (Cu^+, copper decomposition CuD), the position of the HOMO, as well as the HOMO–LUMO gap and population analyses of the anions providing partial charges for all atoms. All these calculations were done in the gas phase. To include media effects the decomposition reactions of a subset of 14 WCAs with the simplest organometallic silylium ion $[SiMe_3]^+$ and the prototype of a metallocene catalyst for olefin polymerization $[Cp_2ZrMe]^+$ were also calculated in the typically employed solvents PhCl and 1,2-$F_2C_6H_4$ (COSMO solvation model). Figure 1 gives an overview of the larger WCAs assessed in this article.

Results

For the sake of readability of the paper for noncomputational chemists, the structures and total energies of the assessed compounds are collected in the appendix at the end of this paper; more extensive discussions can be found in the Supporting Information. One drawing of each optimized compound, together with basic structural parameters and a *xyz* orientation (in Bohr) has been deposited. Readers interested in fine structural details of the optimized species are referred to the Supporting Information.

The size of the necessary calculations with anions containing up to 87 heavy atoms (excluding H) only allowed the use of DFT theory to establish the properties of these species. To obtain data that is more reliable, the assessed quantities were calculated through isodesmic reactions. If some parts of the calculations could not be done isodesmically, higher levels such as MP2/TZVPP, G2, and CBS-Q were used to obtain reliable values for these reactions.

We start this section with the calculation of anchor points for the evaluation of the anion stability before turning to

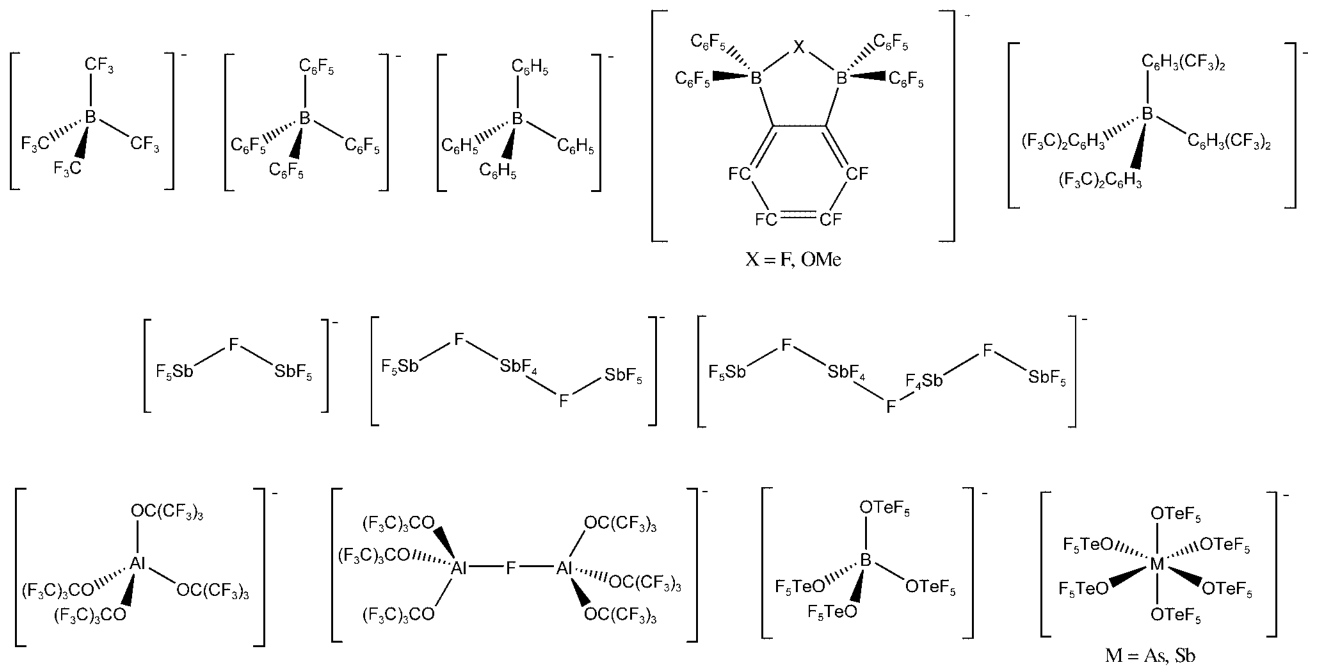

Figure 1. Overview of the larger WCAs assessed in this article.

concepts for the analysis of WCA stability and the examination of solvation effects.

Anchor point I—direct calculation of the FIA of Al_2F_6 with G2 and CBS-Q: To obtain a reliable anchor point for the calculation of the FIA of compounds with fluoride bridges, the structures and total energies of AlF_3 (D_{3h}), AlF_4^- (T_d), Al_2F_6 (D_{2d}), $Al_2F_7^-$ (C_i), OCF_2 (C_{2v}) and OCF_3^- (C_{3v}) were calculated at the G2 and CBS-Q compound levels (Table 1; for total energies, structural parameters, and comment, see Supporting Information). For comparison, the MP2/TZVPP results are also included. With these results the standard enthalpies of reaction for the formation of AlF_4^- and $Al_2F_7^-$ from AlF_3, $2\,AlF_3$, and Al_2F_6 were calculated. For comparison to experimental data,[42] the standard enthalpies of reaction for the formation of $Al_2F_7^-$ from AlF_3 and AlF_4^- as well as the dissociation of Al_2F_6 giving $2\,AlF_3$ were also assessed (Table 1).

Table 1. Standard enthalpies of reaction $\Delta H°$ and reaction energies $\Delta U(0\,K)$ for the formation of $Al_2F_7^-$ and related species (in $kJ\,mol^{-1}$). Experimental enthalpies of reaction $\Delta H°$ for reactions a) and b).[42] Fluoride ion affinities of AlF_3, $2\,AlF_3$, and Al_2F_6 in $kJ\,mol^{-1}$.

Reaction	Exptl[42]	$\Delta U(0\,K)$[a]	$\Delta H°$[b]	$\Delta H°$[c]
a) $Al_2F_6 \rightarrow 2\,AlF_3$	215	205.8	210.4	201.5
b) $AlF_4^- + AlF_3 \rightarrow Al_2F_7^-$	−208[d]	−224.3	−228.0	−226.1
c) $Al_2F_6 + OCF_3^- \rightarrow Al_2F_7^- + OCF_2$	–	−291.8	−286.7	−294.1
d) $2\,AlF_3 + OCF_3^- \rightarrow Al_2F_7^- + OCF_2$	–	−497.6	−497.1	−495.6
e) $AlF_3 + OCF_3^- \rightarrow AlF_4^- + OCF_2$	–	−273.3	−269.1	−269.5
f) $\lvert \Delta H[\text{Eq. c}] \rvert + 209$[e] $= \text{FIA}(Al_2F_6)$	–	500.8	495.7	503.1
g) $\lvert \Delta H[\text{Eq. d}] \rvert + 209$[e] $= \text{FIA}(2\,AlF_3)$	–	706.6	706.1	704.6
h) $\lvert \Delta H[\text{Eq. f}] \rvert + 209$[e] $= \text{FIA}(AlF_3)$	–	482.3	478.1	478.5

[a] MP2/TZVPP. [b] G2. [c] CBS-Q. [d] This value is not very reliable because the errors for the experimental standard enthalpies of formation of AlF_4^- and $Al_2F_7^-$ are quite large (±100 and ±15 $kJ\,mol^{-1}$). [e] The FIA of OCF_2 is 209 $kJ\,mol^{-1}$.

The calculated reaction enthalpies/energies are very similar for all three methods and differ by a maximum of 9 $kJ\,mol^{-1}$ (entry a in Table 1), and the agreement with available experimental data is good. By addition of the FIA of OCF_2 of 209 $kJ\,mol^{-1}$[37] to the enthalpies/energies of entries c–e, the FIAs of AlF_3, $2\,AlF_3$, and Al_2F_6 were obtained (entries f–h). The FIA of AlF_3 of 478–482 $kJ\,mol^{-1}$ is in very good agreement with that obtained at the simpler BP86/SV(P) level (467 $kJ\,mol^{-1}$), which was used for the assessment of the FIAs of the parent Lewis acids of the larger WCAs above.

We will use the average of the FIAs of $2\,AlF_3$ (705 $kJ\,mol^{-1}$) and Al_2F_6 (500 $kJ\,mol^{-1}$) calculated at the most reliable G2 and CBS-Q levels for the evaluation of the FIA of compounds with fluoride bridges (see below).

Anchor point II—direct calculation of the LA of $[F_3AlL]^-$ with MP2/TZVPP and other methods: For the reliable evaluation of the ligand affinity LA of a WCA $[M(L)_n]^-$, the structures of the free ligand L^- and its AlF_3 complex $[F_3AlL]^-$ were calculated at the BP86/SV(P), B3LYP/TZVPP, and MP2/TZVPP levels. As shown above, the MP2/TZVPP, G2, and CBS-Q calculations for the aluminum fluoride species agree within 5 $kJ\,mol^{-1}$. Since the size of the compounds calculated in this section is prohibitive for the application of compound methods such as G2 and CBS-Q, we chose the MP2/TZVPP method as the best applicable level that gives reliable results. To check the quality of the calculations the BP86/SV(P) and selected B3LYP/TZVPP results are also included in Table 2. Next the energies $\Delta U(0\,K)$ of the reaction given in Equation (2) were calculated at these three levels.

Table 2. Reaction energies $\Delta U(0\,K)$ for dissociation of $[F_3AlL]^-$ to L^- and AlF_3 [Eq. (2)] at the BP86/SV(P), B3LYP/TZVPP, and MP2/TZVPP levels (L = $OTeF_5$, C_6H_5, C_6F_5, $C_6H_3(CF_3)_2$, CF_3, OCH_3, $OC(CF_3)_3$).

L^-	BP86[a] [$kJ\,mol^{-1}$]	B3LYP[b] [$kJ\,mol^{-1}$]	MP2[b] [$kJ\,mol^{-1}$]
C_6H_5	433	–	425
$C_6F_5^-$	321	298	315
$C_6H_3(CF_3)_2^-$	395	–	380
CF_3^-	406	355	344
$OC(CF_3)_3^-$	331	298	321
OCH_3^-	472	–	475
$OTeF_5^-$	248	251	273

[a] SV(P) basis set. [b] TZVPP basis set.

$$[F_3AlL]^- \xrightarrow{\Delta U=?} AlF_3 + L^- \qquad (2)$$

Since this reaction is non-isodesmic, it is of importance to check the similarity of the reaction energies with different methods. All calculated reaction energies are listed in Table 2.

Generally, the agreement between the BP86/SV(P) and MP2/TZVPP reaction energies in Table 2 is good and within less than 25 $kJ\,mol^{-1}$. The same holds for the B3LYP and MP2 values. The only exception is the abstraction of the CF_3^- ion at the BP86 level. For the correct energetic description of this species, which has the highest relative fluorine content of all L^- in Table 2, the delocalization of the negative charge is presumably very important. This requires more flexible basis sets than SV(P), as used for the BP86 calculation. The B3LYP and MP2 values with the larger TZVPP basis agree within 11 $kJ\,mol^{-1}$. Similarly, when the reaction energy with $L^- = CF_3^-$ was calculated at the BP86/TZVPP level, it decreased from 406 (SV(P)) to 349 $kJ\,mol^{-1}$, well within the range of the MP2 (344) and B3LYP (355) values. Thus it follows that reaction energies for non-isodesmic reactions with the flexible TZVPP basis are more reliable. Since, in our experience and as shown in the preceding section, the MP2/TZVPP level gives better geometries and energies than the B3LYP/TZVPP level,[31] the MP2/TZVPP values in Table 2 were chosen as the anchor point for the calculation of the ligand affinity LA below.

Concepts for analyzing the stability and coordinating ability of a WCA on computational grounds: With the following reasonable suggestions the relative stability and coordinating ability of the WCAs were compared:

1) All anions that are based on a Lewis acidic central atom are prone to ligand abstraction as a decomposition reac-

tion.[1d] A measure for the intrinsic stability of a given WCA is the Lewis acidity of the parent Lewis acid A, for example, $B(C_6F_5)_3$ for the $[B(C_6F_5)_4]^-$ ion. A firmly established measure for Lewis acidity is the fluoride ion affinity FIA calculated through an isodesmic reaction [Eq. (3)]:[37]

$$\begin{array}{l} A + OCF_3^- \xrightarrow[\text{BP86/SVP}]{\text{isodesmic,}} AF^- + OCF_2 \\ OCF_2 + F^- \xrightarrow[\text{experimental value}]{} OCF_3^- \\ \hline A + F^- \xrightarrow{-\Delta H = \text{FIA}} AF^- \qquad (3) \end{array}$$

We calculated the FIAs according to this known[37] scheme, and all FIAs of the parent Lewis acids A of the WCAs examined are included in Table 5 below. The previously established[37] anchor point for this scale is the experimental FIA of OCF_2 of 209 kJ mol^{-1}. The higher the FIA of A, the more stable is the respective WCA towards ligand abstraction. For comparison, the FIAs calculated[37] by Christe and Dixon are also included in Table 5 below.

The approach as in Equation (3) works very well as long as the WCAs do not contain fluoride bridges. In this case the reactions are non-isodesmic, and therefore additional calculations had to be performed to allow a reliable evaluation of the FIA of the parent Lewis acids of these WCAs. To evaluate the FIA of Sb_nF_{5n} ($n = 2, 3, 4$) giving the fluoride bridged anions $[Sb_nF_{5n+1}]^-$ ($n = 2, 3, 4$) the FIA was calculated by two separate calculations:

- The FIA of the doubly fluoride bridged Al_2F_6 (D_{2h}) giving the singly fluoride bridged $Al_2F_7^-$ ion was calculated on the basis of the average of G2 and CBS-Q calculations as 500 kJ mol^{-1}. This step is non-isodesmic, but the G2 and CBS-Q levels are reported[62,63] to reproduce experimental values with a uncertainty of less than 8 kJ mol^{-1}, lending credibility to these values.
- The FIAs of Sb_nF_{5n} ($n = 2, 3, 4$) were then calculated for an isodesmic reaction of $Al_2F_7^-$ and Sb_nF_{5n} giving $[Sb_nF_{5n+1}]^-$ and Al_2F_6 by adding the reaction enthalpy of the latter reaction to the FIA of Al_2F_6 of 500 kJ mol^{-1}, that is, Equation (4) for $[Sb_2F_{11}]^-$.

$$\begin{array}{l} Sb_2F_{10} + Al_2F_7^- \xrightarrow[\text{BP86/SVP}]{\text{isodesmic,}} Sb_2F_{11}^- + Al_2F_6 \\ Al_2F_6 + OCF_3^- \xrightarrow[\text{(G2 + CBS-Q)/2}]{\text{non isodesmic,}} Al_2F_7^- + OCF_2 \\ OCF_2 + F^- \xrightarrow[\text{experimental value}]{} OCF_3^- \\ \hline Sb_2F_{10} + F^- \xrightarrow{-\Delta H = \text{FIA}} Sb_2F_{11}^- \qquad (4) \end{array}$$

Similarly the FIAs of $[(RO)_3AlFAl(OR)_3]^-$ and $[F_4C_6\{1,2\text{-}\{B(C_6F_5)_2\}_2\}F]^-$ were assessed in isodesmic reactions of $Al_2F_7^-$ and the Lewis acids $2\,Al(OR)_3$ and $F_4C_6\{1,2\text{-}\{B(C_6F_5)_2\}_2\}$ giving $2\,AlF_3$ and the fluoride-bridged anion. From this reaction energy and the FIA of $2\,AlF_3$, calculated on the basis of the average of G2 and CBS-Q calculations of -705 kJ mol^{-1}, the FIA of $2\,Al(OR)_3$ and $F_4C_6\{1,2\text{-}\{B(C_6F_5)_2\}_2\}$ followed, that is, Equation (5) for $[(RO)_3AlF\text{-}Al(OR)_3]^-$.

$$\begin{array}{l} 2\,Al(OR)_3 + Al_2F_7^- \xrightarrow[\text{BP86/SVP}]{\text{isodesmic,}} (RO)_3Al\text{-}F\text{-}Al(OR)_3^- + 2\,AlF_3 \\ 2\,AlF_3 + OCF_3^- \xrightarrow[\text{(G2 + CBS-Q)/2}]{\text{non isodesmic,}} Al_2F_7^- + OCF_2 \\ OCF_2 + F^- \xrightarrow[\text{experimental value}]{} OCF_3^- \\ \hline 2\,Al(OR)_3 + F^- \xrightarrow{-\Delta H = \text{FIA}} (RO)_3Al\text{-}F\text{-}Al(OR)_3^- \qquad (5) \end{array}$$

2) Additionally, we also directly assessed the ligand affinity LA of all types of WCAs. The LA is the enthalpy of reaction necessary to remove the anionic ligand L^- from the anion $[M(L)_n]^-$ [Eq. (6)].

$$M(L)_n^- \xrightarrow{\Delta H = \text{LA}} M(L)_{n-1} + L^- \qquad (6)$$

The LA was partitioned into two parts: the first was an isodesmic reaction that also allowed reliable calculations for very large systems at the DFT level BP86/SV(P). The second reaction contains much smaller species, but is non-isodesmic. Therefore, the computationally much more expensive, but also more reliable, MP2/TZVPP level was selected to assess the second part. The LA was then obtained by a simple addition of the two equations [Eq. (7)].

$$\begin{array}{l} M(L)_n^- + AlF_3 \xrightarrow[\text{BP86/SVP}]{\text{isodesmic,}} M(L)_{n-1} + F_3Al\text{-}L^- \\ F_3Al\text{-}L^- \xrightarrow[\text{MP2/TZVPP}]{\text{non isodesmic,}} AlF_3 + L^- \\ \hline M(L)_n^- \xrightarrow{\Delta H = \text{LA}} M(L)_{n-1} + L^- \qquad (7) \end{array}$$

The LA is always endothermic, and the larger the positive LA value in Table 5, the more stable is the WCA versus ligand abstraction. However, a word of caution is needed here: The LA also reflects the stability of the generated L^- ion. Thus, if L^- is stable, like $L^- = OC(CF_3)_3^-$ or $OTeF_5^-$, the LA is relatively low compared to less stable anionic ligands such as $L^- = C_6H_5^-$ or $C_6H_3(CF_3)_2^-$.

3) To assess the stability of a WCA towards attack of a hard or soft electrophile and to eliminate the contribution of the intrinsic stability of L^- in 2), the isodesmic decomposition reactions of $[M(L)_n]^-$ with H^+ [hard, Eq. (8)] and Cu^+ [soft, Eq. (9)] were calculated in which PD stands for proton decomposition, and CuD for copper decomposition.

$$\mathrm{M(L)}_n^- + \mathrm{H}^+ \xrightarrow{\Delta H = \mathrm{PD}} \mathrm{M(L)}_{n-1} + \mathrm{HL} \quad (8)$$

$$\mathrm{M(L)}_n^- + \mathrm{Cu}^+ \xrightarrow{\Delta H = \mathrm{CuD}} \mathrm{M(L)}_{n-1} + \mathrm{CuL} \quad (9)$$

The PD and CuD allow conclusions to be drawn on the stability of a given WCA of type $[\mathrm{M(L)}_n]^-$ upon reaction with a hard (H^+, PD) or soft (Cu^+, CuD) electrophile. Since a gaseous anion and a gaseous cation react in Equations (8) and (9) to give two neutral species, PD and CuD are both exothermic. The less negative the PD and CuD values in Table 5 are, the more stable is the WCA against electrophilic attack. For gas-phase acidities of neutral Brønsted acids including $\mathrm{H[CB_{11}F_{12}]}$, see reference [43].

4) The energy of the HOMO of a WCA is related to its resistance towards oxidation. The lower the HOMO energy, the more difficult it is to remove an electron and thus to oxidize the WCA.

5) The HOMO–LUMO gap in Table 5 can be associated with the resistance of an anion towards reduction, and the larger the gap, the more stable the anion is with respect to reduction. Very small gaps such as those for $[\mathrm{Sb_4F_{21}}]^-$ or $[\mathrm{As(OTeF_5)_6}]^-$ are an indication of the potentially oxidizing character of these anions, which may interfere with countercations sensitive towards oxidation.

6) As a measure for the coordinating ability of an anion the partial charges of the most negatively charged atom (q_{neg}) and most negatively charged surface atom (q_{surf}) are collected in Table 5 (see later). Clearly, low charges are an indication for low coordination ability. However, steric effects may also be of importance, and the most basic atoms may be hidden in the center of a large WCA and therefore unavailable for coordination. In this case, the charge of the most basic accessible surface atoms q_{surf} appears to be a better measure.

Reactions with $\mathrm{SiMe_3}^+$ and $[\mathrm{Cp_2ZrMe}]^+$: To illustrate the meaning of abstract quantities such as FIA, LA, PD, and CuD, we explicitly calculated reactions of the examined anions with two common reactive counterions: $\mathrm{SiMe_3}^+$ as the simplest organometallic silylium ion, and $[\mathrm{Cp_2ZrMe}]^+$ as the prototype for all zirconocene-based olefin polymerization catalysts. To account for effects of the reaction medium, we also calculated the respective solvation enthalpies with the COSMO model at the BP86/SV(P) level. The total energies and COSMO solvation energies for $\mathrm{SiMe_3}^+$, $[\mathrm{Cp_2ZrMe}]^+$, $\mathrm{LSiMe_3}$, and $[\mathrm{Cp_2Zr(Me)L}]$ in PhCl ($\varepsilon_r = 5.69$), and 1,2-$\mathrm{F_2C_6H_4}$ ($\varepsilon_r = 13.38$) as solvents can be found in the Supporting Information. Since two ions react with formation of two neutral molecules, solvation effects are crucial for the sign of the decomposition enthalpy.

Reactions with $\mathrm{SiMe_3}^+$: The free $\mathrm{SiMe_3}^+$ ion is unknown in condensed phases, but its arene adduct is accessible. Free simple $\mathrm{SiR_3}^+$ (R = Me, Et, etc.) silylium ions either coordinate or decompose the counterions. The only structurally characterized example of a free and truly tricoordinate silylium ion is the more bulkily substituted $\mathrm{SiMes_3}^+$ ion (Mes = 2,4,6-$\mathrm{Me_3C_6H_2}$) partnered with the $[\mathrm{CB_{11}Cl_6Me_5H}]^-$ ion.[23] However, it is known that this cation is also moderately stable with the $[\mathrm{B(C_6F_5)_4}]^-$ ion. For an overview on the literature before 1998, see reference [44]. With this background, it is instructive to analyze Table 3, in which all reaction energies in the gas phase and in solution according to Equation (10) are collected.

$$[\mathrm{M(L)}_n]^- + \mathrm{SiMe}_3^+ \xrightarrow{\Delta_r H = ?} \mathrm{L\text{-}SiMe_3} + \mathrm{M(L)}_{n-1} \quad (10)$$

Table 3. Reaction energies in the gas phase (g) and in solution in PhCl ($\varepsilon_r = 5.69$) and 1,2-$\mathrm{F_2C_6H_4}$ ($\varepsilon_r = 13.38$) according to Equation (10).

Anion	$\Delta_r U$(g)	$\Delta_r U_{\mathrm{PhCl}}$	$\Delta_r U_{1,2\text{-}\mathrm{F_2C_6H_4}}$
$\mathrm{BF_4}^-$	−622	−272	−210
$\mathrm{PF_6}^-$	−566	−228	−168
$\mathrm{AsF_6}^-$	−534	−203	−145
$\mathrm{SbF_6}^-$	−471	−164	−109
$\mathrm{Sb_2F_{11}}^-$	−437	−149	−98
$\mathrm{Sb_3F_{16}}^-$	−404	−140	−93
$\mathrm{Sb_4F_{21}}^-$	−402	−145	−100
$[\mathrm{B(OTeF_5)_4}]^-$	−404	−157	−114
$[\mathrm{As(OTeF_5)_6}]^-$	−388	−144	−102
$[\mathrm{Sb(OTeF_5)_6}]^-$	−337	−94	−52
$[\mathrm{Al(OR)_4}]^-$[a]	−400	−142	−96
$[\mathrm{(RO)_3AlFAl(OR)_3}]^-$[a]	−301 (−379)[b]	−65	−23
$[\mathrm{B(C_6F_5)_4}]^-$	−488	−232	−187
$[\mathrm{B(CF_3)_4}]^-$	−348	−49	+5

[a] R = $\mathrm{C(CF_3)_3}$. [b] Kinetic (thermodynamic) value, that is, isomer I (isomer II) (see Appendix).

Since the number of particles on each side of Equation (10) is the same, entropy is not expected to change the reaction energies. All anions except for the smaller $[\mathrm{B(CF_3)_4}]^-$ in the most polar solvent 1,2-$\mathrm{F_2C_6H_4}$ are incompatible with the reactive $\mathrm{SiMe_3}^+$ ion.

Reactions with $[\mathrm{Cp_2ZrMe}]^+$: To achieve living polymerization and high catalytic activity, the zirconocenium catalyst should be long lived, and thus many efforts were made to keep the anion out of the active site of the cationic catalyst.[1c,d] The reactive $[\mathrm{Cp_2ZrMe}]^+$ ion is the prototype of this kind of catalyst,[1c,d] and therefore we were interested in understanding whether the stability of the mainly used $[\mathrm{B(C_6F_5)_4}]^-$ and related WCAs is thermodynamic or kinetic and how other types of WCAs compare to the $[\mathrm{B(C_6F_5)_4}]^-$ ion. Therefore, the decomposition as in Equation (11) was analyzed (Table 4).

$$[\mathrm{ML}_n]^- + [\mathrm{Cp_2ZrMe}]^+ \xrightarrow{\Delta_r H = ?} [\mathrm{Cp_2Zr(Me)L} + \mathrm{ML}_{n-1} \quad (11)$$

Similar to Equation (10), the number of particles on both sides of Equation (11) is the same and, therefore, entropy is not expected to change the reaction energies. From Table 4 one notes that $[\mathrm{Cp_2ZrMe}]^+$ is less electrophilic than $\mathrm{SiMe_3}^+$, but the majority of the solution decomposition reactions are still exothermic, that is, the stability of catalysts with, for example, $\mathrm{B(C_6F_5)_4]^-}$ as a WCA is kinetic. The formation of a Zr–C bond appears to be less favorable than that of a Si–C bond, and thus WCAs in which a Zr–C bond is formed during decomposition (i.e., $[\mathrm{B(C_6F_5)_4}]^-$, $[\mathrm{B(CF_3)_4}]^-$) perform much better than in the reaction with $\mathrm{SiMe_3}^+$. Still there are

Table 4. Reaction energies in the gas phase (g) and in solution in PhCl ($\varepsilon_r = 5.69$) and 1,2-$F_2C_6H_4$ ($\varepsilon_r = 13.38$) according to Equation (11).

Anion	Δ_rU(g)	Δ_rU_{PhCl}	$\Delta_rU_{1,2\text{-}F_2C_6H_4}$
BF_4^-	−542	−215	−155
PF_6^-	−486	−170	−113
AsF_6^-	−454	−146	−90
SbF_6^-	−391	−106	−55
$Sb_2F_{11}^-$	−356	−92	−44
$Sb_3F_{16}^-$	−324	−83	−39
$Sb_4F_{21}^-$	−322	−88	−45
$[B(OTeF_5)_4]^-$	−346	−117	−76
$[As(OTeF_5)_6]^-$	−330	−104	−64
$[Sb(OTeF_5)_6]^-$	−279	−55	−14
$[Al(OR)_4]^-$[a]	−347	−107	−63
$[(RO)_3AlFAl(OR)_3]^-$[a]	−249 (−171)[b]	−30	+10
$[B(C_6F_5)_4]^-$	−353	−118	−75
$[B(CF_3)_4]^-$	−214	+64	+115

[a] $R = C(CF_3)_3$. [b] Kinetic (thermodynamic) value, that is, isomer I (isomer II) (see Appendix).

other easily accessible WCAs, such as $[Al(OR)_4]^-$, which have the same stability as the most frequently employed WCAs (i.e., $[B(C_6F_5)_4]^-$).

Discussion

Stability and coordinating ability of the WCAs based on LA, FIA, PD, CuD, HOMO level, HOMO–LUMO gap, and partial charges: Ligand abstraction[45–48] and hydrolysis are frequently observed decomposition pathways for WCAs, and, therefore, the computational approach to calculate LA, PD, and CuD mimics experimental observations. Examples of ligand abstraction include reactions of $SiPh_3^+$ with $[B(OTeF_5)_4]^-$,[45] and $[Me(Ph_3P)_2Pt(OEt_2)]^+[B(Ar^F)_4]^-$ ($Ar^F = C_6H_3(CF_3)_2$);[46] also the $[B(C_6F_5)_4]^-$ ion rapidly degrades in the presence of AlR_2^+,[48] RZn^+,[47] and H^+ ions (R = Me, Et) if no donor solvent is present (e.g., OEt_2). However, by calculations only the underlying thermodynamics can be assessed, and kinetic barriers against decomposition may additionally stabilize a given WCA (see $Al_2(OR)_5F$ structure below). Also decomposition pathways other than ligand abstraction may occur; this was, for example, recently shown for the $[B(CF_3)_4]^-$ ion.[1d,41] The data included in Table 5 cannot be taken as absolute, but since the same methods were used for all calculations, relative trends will definitely be correct. For the carborane-based anions the FIA, LA, PD, and CuD cannot directly be assessed, and, therefore, these WCAs were excluded from this approach. All calculated values are collected in Table 5.

Table 5 reveals the outstanding capability of the $[Sb_3F_{16}]^-$, $[Sb_4F_{21}]^-$, and $[Sb(OTeF_5)_6]^-$ WCAs to stabilize highly oxidizing cations even in anhydrous HF (see FIA, PD, HOMO level). This stability versus oxidation must be traded for sensitivity to reduction (see gap in Table 5). Moreover, the fluoroantimonates and teflate anions are extremely moisture sensitive and decompose in the presence of traces of water in glassware with autocatalytic formation of HF that reacts with SiO_2 to form SiF_4 and H_2O, which re-enters the cycle. This sensitivity towards moisture allows the use of these WCAs in only a few laboratories worldwide. In terms of coordinating ability, these WCAs are more coordinating than others (cf. q_{bas} and q_{surf}).

For the borate-based anions it can be seen from Table 5 that fluorination greatly increases the thermodynamic stability of all fluorinated borates relative to the nonfluorinated $[B(C_6H_5)_4]^-$ ion (see FIA, LA, PD, CuD, HOMO level, gap). The differences between the commercially available $[B(C_6F_5)_4]^-$ and $[B(C_6H_3(CF_3)_2)_4]^-$ WCAs are small, but diborane-based anions such as $[F_4C_6\{1,2\text{-}\{B(C_6F_5)_2\}_2\}X]^-$ (X=

Table 5. Calculated properties of WCAs: FIA of the parent Lewis acid; LA, PD, and CuD of the WCA; position of the HOMO of the WCA [eV]; HOMO–LUMO gap of the WCA [eV]; partial charge of the most negatively charged atom q_{neg}; and partial charge of the most negatively charged surface atom q_{surf}.

Anion	Symmetry	FIA [kJ mol^{-1}]	FIA[37] [kJ mol^{-1}]	LA [kJ mol^{-1}]	PD [kJ mol^{-1}]	CuD [kJ mol^{-1}]	HOMO [eV]	Gap [eV]	q_{neg}	q_{surf}
BF_4^-	T_d	338	348[37]	–[a]	−1212	−521	−1.799	10.820	−0.25 F	−0.25 F
PF_6^-	D_{4h}	394	397[37]	–[a]	−1156	−465	−2.672	8.802	−0.44 F	−0.44 F
AsF_6^-	D_{4h}	426	443[37]	–[a]	−1124	−433	−3.149	6.284	−0.44 F	−0.44 F
SbF_6^-	D_{4h}	489	503[37]	–[a]	−1061	−371	−3.911	5.135	−0.44 F	−0.44 F
$Sb_2F_{11}^-$ vs Sb_2F_{10}	C_1	549	–	–[a]	−1026	−336	−5.540	4.336	−0.40 F	−0.40 F
$Sb_3F_{16}^-$ vs Sb_3F_{15}	C_i	582	–	–[a]	−994	−303	−6.342	3.886	−0.38 F	−0.38 F
$Sb_4F_{21}^-$ vs Sb_4F_{20}	C_{2v}	584	–	–[a]	−991	−301	−6.579	3.256	−0.39 F	−0.39 F
$[B(OTeF_5)_4]^-$	C_1	550	–	274	−1040	−420	−5.811	2.593	−0.40 F	−0.40 F
$[As(OTeF_5)_6]^-$	C_3	593	–	290	−1023	−403	−6.335	2.204	−0.62 O	−0.40 F
$[Sb(OTeF_5)_6]^-$	C_3	633	–	341	−973	−353	−6.610	2.326	−0.61 O	−0.39 F
$[Al(OR)_4]^-$ ($R = C(CF_3)_3$)	S_4	537	–	342	−1081	−395	−4.100	6.747	−0.24 O	−0.20 F
$[(RO)_3AlFAl(OR)_3]^-$[b,e]	C_i	685[b]	–	441 (363)	−983 (−1061[e])	−297 (−375[e])	−4.987	6.500	−0.23 O	−0.20 F
$[B(C_6H_5)_4]^-$	S_4	342	–	324	−1402	−649	−2.150	4.087	−0.45 B	−0.05 H
$[B\{C_6H_3(CF_3)_2\}_4]^-$	S_4	471	–	382	−1251	−506	−3.789	3.816	−0.44 B	−0.22 F
$[B(C_6F_5)_4]^-$	S_4	444	–	296	−1256	−538	−3.130	4.196	−0.21 F	−0.21 F
$[B(CF_3)_4]^-$	T	552	–	490	−1136	−379	−3.530	9.158	−0.58 B	−0.21 F
$[F_4C_6\{1,2\text{-}\{B(C_6F_5)_2\}_2\}F]^-$[c]	C_1	510	–	328[c]	−1224[c]	−506[c]	−3.274	3.861	−0.54 B	−0.22 F
$[F_4C_6\{1,2\text{-}\{B(C_6F_5)_2\}_2\}OMe]^-$[d]	C_1	510	–	586[d]	−1061[d]	−332[d]	−3.101	3.754	−0.68 B	−0.22 C
$[F_4C_6\{1,2\text{-}\{B(C_6F_5)_2\}_2\}OMe]^-$[c]	C_1	–	–	305[c]	−1247[c]	−529[c]	–	–	–	–

[a] LA and FIA are identical. [b] FIA vs 2 $Al(OR)_3$ ($R = C(CF_3)_3$). [c] Against $C_6F_5^-$ (LA) or EC_6F_5 abstraction (E = H: PD, E = Cu: CuD). [d] Against OMe^- (LA) or EOMe abstraction (E = H: PD, E = Cu: CuD). [e] Values in parentheses correspond to the formation of $Al_2(OR)_5F$ isomer I (see text) ($R = C(CF_3)_3$).

F, OMe) are even more stable WCAs. Of all borates the novel $[B(CF_3)_4]^-$ ion is the most stable with respect to the examined decomposition pathways. However, see reference [41] for an experimental investigation of other decomposition pathways.

The stability of the perfluoroalkoxyaluminate $[Al(OR)_4]^-$ ($R = C(CF_3)_3$) with respect to FIA, PD, CuD, HOMO level, and gap in Table 5 is remarkable and higher than that of all borates except the $[B(CF_3)_4]^-$ ion, which has comparable values. The $[Al(OR)_4]^-$ ion even comes close to the oxidation resistance and low PDs of the fluoroantimonates and is in part even better than those of the teflate-based anions. In contrast to the last two types of anions, the synthesis of the perfluoroalkoxyaluminate $[Al(OR)_4]^-$ is straightforward and can be performed in conventional inorganic laboratories worldwide. This shows the great potential of this special type of anion for chemistry. An even better choice would be the fluoride bridged $[(RO)_3AlFAl(OR)_3]^-$ ion, which is among the best WCAs according to each entry in Table 5, but this WCA is only known as a decomposition product.[31] However, we recently established a direct synthesis of a silver salt of this WCA.[49] For other new, fluoride-bridged aluminates, see reference [7d].

Inclusion of solvation enthalpies: Silylium and zirconocenium ions are two prominent examples for the application of WCAs to stabilize reactive cations. To compare the relative stabilities of WCAs $[M(L)_n]^-$, we analyzed their decomposition reactions with $SiMe_3^+$ and $[Cp_2ZrMe]^+$ as reactive counterion in the gas phase and in solution [PhCl and 1,2-$F_2C_6H_4$, see Eqs. (10) and (11)].

Gas-phase values versus (calculated) solution values—are solvation energies necessary to evaluate the WCAs?: In this section, we investigate the extent to which the gas-phase data in Table 5 can be transferred to reactions in solution. To illustrate this point we plotted the solvation reaction energies Δ_rU of Equations (10) and (11) in PhCl and 1,2-$F_2C_6H_4$ against the FIA of the respective WCA in the gas phase (Figure 2).

Figure 2 shows that a roughly linear relationship exists between the FIA in the gas phase and the reaction energies Δ_rU in solution. This is taken as clear evidence that the results obtained from gas-phase calculations (i.e., those in Table 5) can be used to extract meaningful answers for reactions in solution. The only exception from this notion is found for the relatively small $[B(CF_3)_4]^-$ ion (see below for reasons).

Relative stabilization by solvation: The extent to which a reaction is stabilized by solvation enthalpies is analyzed in Figure 3. Here the stabilization $\Delta(\Delta_rU)$ of the gas-phase reaction by solvation enthalpies in the most polar solvent 1,2-$F_2C_6H_4$, that is, $\Delta(\Delta_rU) = \Delta_rU(g) - \Delta_rU(1,2\text{-}F_2C_6H_4)$, was plotted against the number of atoms of the anion, which was taken as a measure of its size and thus also for the absolute value of the solvation enthalpy, which is roughly inversely proportional to the ionic radius (e.g., see the simple Born equation). Thus, reactions with smaller anions are expected to be more stabilized by solvation enthalpies than those with larger anions (Figure 3).

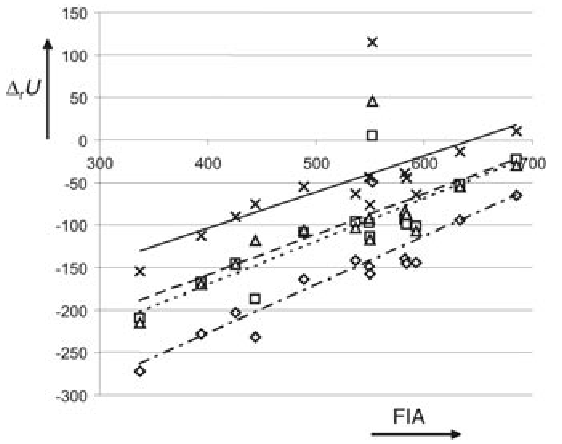

Figure 2. Solvation reaction energies Δ_rU of Equations (10) and (11) in PhCl and 1,2-$F_2C_6H_4$ versus the FIA of the respective WCA in the gas phase. ◇: Equation (10) in PhCl; □: Equation (10) in 1,2-$F_2C_6H_4$; △: Equation (11) in PhCl; ×: Equation (11) in 1,2-$F_2C_6H_4$.

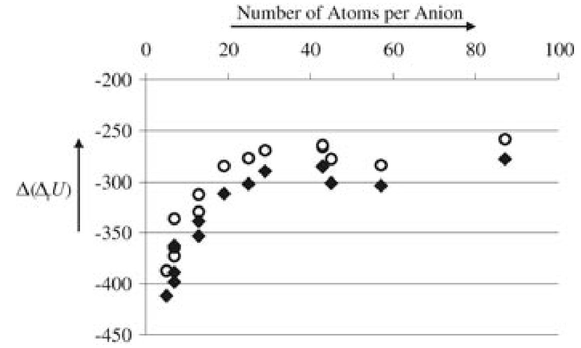

Figure 3. Stabilization of reactions by solvation enthalpy. $\Delta(\Delta_rU(g) - \Delta U(1,2\text{-}F_2C_6H_4))$: ◆ Equation (10), ○ Equation (11).

For small anions such as BF_4^- and PF_6^- the stabilization $\Delta(\Delta_rU)$ is large and may approach 400 kJ mol^{-1}; with increasing anion size, the relative stabilization decreases quickly to about 250–300 kJ mol^{-1}. Remarkably, starting from an anion size of about 25 atoms, the stabilization by solvation remains almost constant and only adds a constant value to the gas-phase reaction energy. This may also be seen from Figures 4 and 5, in which the gas-phase and solution reaction energies of Equations (10) and (11) are plotted for all WCAs.

From the preceding, we learn the following: 1) For larger WCAs exceeding about 25 atoms the most important input for the stabilization of a reactive cation in a given solvent is its stability against ligand abstraction. To assess the anion stability gas phase values such as FIA, PD or CuD can also be used. 2) The best solution for stabilizing a given reactive cation would be a very small WCA that is very stable against ligand abstraction and very weakly coordinating so that competition with anion coordination is excluded. Probably one of the best compromises in this respect is the $[B(CF_3)_4]^-$ ion; however, very recently other decomposition reactions of this anion were found[41] and show that this

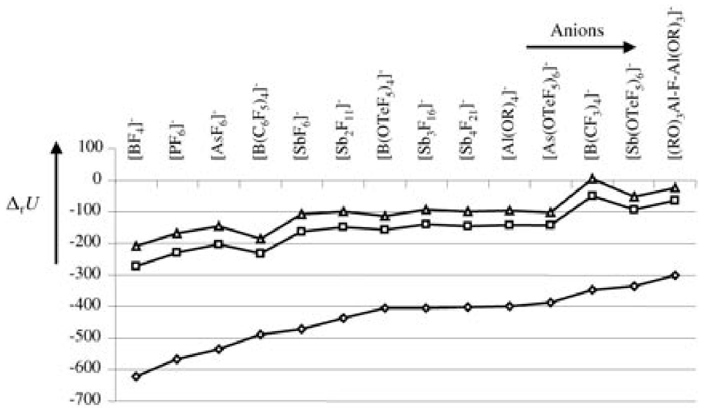

Figure 4. Gas-phase and solution reaction energies of Equation (10). △: in 1,2-$F_2C_6H_4$; □: in PhCl; ◇: gas phase.

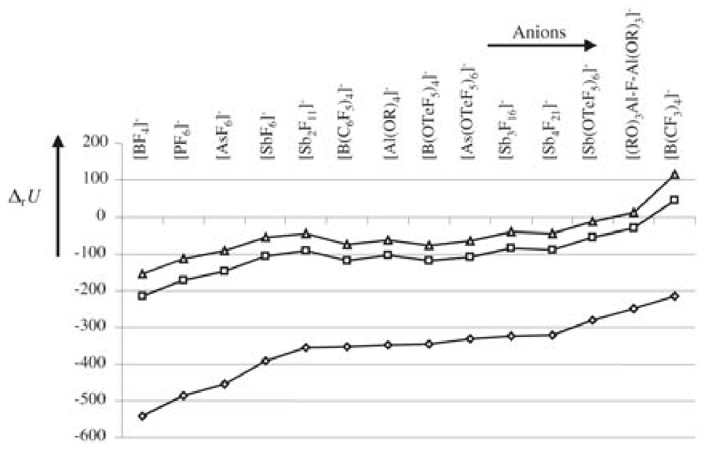

Figure 5. Gas-phase and solution reaction energies of Equation (11). △: in 1,2-$F_2C_6H_4$; □: in PhCl; ◇: gas phase.

anion is not as ideal for stabilizing reactive cations as might be anticipated from the data in Table 5.

Using the data in Table 5—prediction of reactions: Especially the FIA and LA in Table 5 are valuable tools for predicting the outcome of hitherto unknown reactions.

Application of the LA—assessment of WCA stability in the presence of a target cation: With some small extra calculations or estimations, the LA in Table 5 can also be used to assess the stability of a WCA in the presence of a reactive target cation. Let us consider the carbene-analogous PCl_2^+ ion as an example for a desired reactive target cation and the WCA $[Al(OR)_4]^-$ as the counterion [i.e., the decomposition as in Eq. (12)].

$$PCl_2^+ + [Al(OR)_4]^- \rightarrow ROPCl_2 + Al(OR)_3 \qquad (12)$$

The first step is to calculate the target cation and the neutral species resulting from the reaction of the cation and the anion, that is, PCl_2^+ and $ROPCl_2$. If the (affordable) BP86/SV(P) level is chosen, one can use Equation (12) and the total energies of $[Al(OR)_4]^-$ and $Al(OR)_3$ given in this article to directly calculate the (isodesmic) gas-phase reaction energy of Equation (12) as $-447\,kJ\,mol^{-1}$. However, if other, for example, higher correlated methods are used, the next step is to separate Equation (12) into two parts [Eq. (13) and LA].

$$PCl_2^+ + OR^- \xrightarrow{\Delta_rU = -789} RO\text{-}PCl_2 \qquad (13)$$

$$[Al(OR)_4]^- \xrightarrow{LA = 342} RO^- + Al(OR)_3 \qquad (LA)$$

$$PCl_2^+ + [Al(OR)_4]^- \xrightarrow{\Delta_rU = -447} RO\text{-}PCl_2 + Al(OR)_3 \qquad (12)$$

Equation (13) can be calculated directly, but an isodesmic route is more accurate.[50] Adding Equation (13) and the LA gives the desired gas-phase reaction energy of Equation (12) as $-447\,kJ\,mol^{-1}$. Thus, with two relatively small calculations and the data from this article, the stability of the 18 WCAs collected here with a desired target cation in the gas phase can be checked. Equation (12) contains two particles on both sides, so entropy can be neglected, but since two ions react to form two neutral species, solvation should be taken into account. Thus, to examine whether the salt PCl_2^+ $[Al(OR)_4]^-$ is stable in PhCl or 1,2-$F_2C_6H_4$ solution, the COSMO solvation enthalpies of PCl_2^+ and $ROPCl_2$ must be calculated at the BP86/SV(P) level. Together with the COSMO solvation enthalpies of $[Al(OR)_4]^-$ and $Al(OR)_3$ included in this article, next the solution stability of Equation (12) was assessed. As expected, solvation greatly stabilizes Equation (12) in PhCl by $291\,kJ\,mol^{-1}$ and in 1,2-$F_2C_6H_4$ by $343\,kJ\,mol^{-1}$, but in both solvents the decomposition is still considerably favorable (by -157 and $-104\,kJ\,mol^{-1}$, respectively). This is in line with recent experiments that showed that the PCl_2^+ ion, generated from $Ag^+[Al(OR)_4]^-$ and PCl_3, completely decomposed the $[Al(OR)_4]^-$ ion.[49] However, the analysis for the fluoride-bridged $[(RO)_3AlFAl(OR)_3]^-$ as WCA in Equation (12) shows that the gas-phase reaction is only unfavorable by $-348\,kJ\,mol^{-1}$, and by $-31\,kJ\,mol^{-1}$ when solvation is taken into account in the most polar solvent; this suggests that the PCl_2^+ ion may be marginally stable with this WCA in solution at low temperature.

Estimating the success of fluoride ion abstraction: synthesis of $FCO^+[X]^-$ as a target salt: With the FIAs collected in Table 5 fluoride ion abstractions can be planned. A likely candidate for such a reaction is the formation of a OCF^+ salt from OCF_2 and a Lewis acid. As example in Equation (14) we selected the $M(OTeF_5)_5$ Lewis acids (M = As, Sb), which—although the antimony representative is very unstable—are the strongest monomeric Lewis acids known (see Table 5). Equation (14) also has two particles on each side, and therefore entropy is not important.

The reaction energy of Equation (15) is most accurately obtained by an isodesmic reaction (see ref. [51]), and with the small effort of calculating OCF^+, OCF_2, and OCF_3^- as well as taking the FIA of $M(OTeF_5)_5$ (Table 5), one can estimate that Equation (14) is unfavorable in the gas phase by 483 (As) or $443\,kJ\,mol^{-1}$ (Sb). To account for the important

$$\mathrm{M(OTeF_5)_5} + \mathrm{F^-} \xrightarrow{\Delta_rU = -593/-633\ \mathrm{kJ\,mol^{-1}}} [\mathrm{F\text{-}M(OTeF_5)_5}]^- \qquad \text{(FIA)}$$

$$\mathrm{F_2CO} \xrightarrow{\Delta_rU = 1076\ \mathrm{kJ\,mol^{-1}}} \mathrm{FCO^+} + \mathrm{F^-} \qquad (15)$$

$$\overline{\mathrm{M(OTeF_5)_5} + \mathrm{F_2CO} \xrightarrow{\Delta_rU = +483/+443\ \mathrm{kJ\,mol^{-1}}} \mathrm{FCO^+} + [\mathrm{F\text{-}M(OTeF_5)_5}]^- \qquad (14)}$$

solvation effects, the COSMO solvation enthalpies of F_2CO and FCO^+ were calculated; those of $M(OTeF_5)_5$ and $[FM(OTeF_5)_5]^-$ were taken from the Supporting Information of this paper. Then the reaction energy of Equation (14) in the most polar solvent ($\varepsilon_r = 13.38$) followed as +98 (As) and +58 $\mathrm{kJ\,mol^{-1}}$ (Sb). This estimate suggests that the salt $OCF^+[FM(OTeF_5)_5]^-$ is not a promising target for synthesis in solvents of this polarity.[52] A weakly basic and more polar solvent with $\varepsilon_r > 14$ may promote the formation of dissolved $OCF^+[FSb(OTeF_5)_5]^-$ due to the higher solvation enthalpies for the ions. From the preceding it appears unlikely to prepare a FCO^+ salt in solution with the Lewis acids in Table 5. This conclusion is in agreement with previous unsuccessful attempts to prepare FCO^+ salts by reaction of F_2CO with even a large excess of MF_5 (M = As, Sb).[53] However, it was found that the less reactive $ClCO^+$ can be obtained from FClCO and Sb_3F_{15}.[53,54] Similar to the above procedure for FCO^+ we estimated the reaction energy for the reaction of Sb_3F_{15} with ClFCO to give $ClCO^+[Sb_3F_{16}]^-$ as favorable in solution by $-15\ \mathrm{kJ\,mol^{-1}}$, which is in good agreement with the experiment and lends support to the predictive power of the data collected in this article (see Supporting Information).

Conclusion

The FIA, LA, PD, CuD, HOMO level, HOMO–LUMO gap, and partial charges of a large group of representative good WCAs were calculated (Table 5). Analysis of the calculated data showed that there is no simple "best anion", and that a decision for a particular anion must be based on several criteria. Some anions are more stable towards soft electrophiles (see CuD) and others towards hard electrophiles (see PD). In terms of coordinating abilities, the fluorinated organoborates and alkoxyaluminates are clearly less coordinating than all fluorometallates or teflate-based anions (see q_{bas} and q_{surf}). Media effects, that is, solvation enthalpies, are important, but from an anion size of about 25 atoms upwards, solvation only adds a constant factor to the gas-phase reaction energy. The calculated solution decomposition reaction energies with $SiMe_3^+$ and $[Cp_2ZrMe]^+$ in PhCl and 1,2-$F_2C_6H_4$ showed that the frequently used $[B(C_6F_5)_4]^-$ counterion is thermodynamically unstable with these cations and that the observed (small) solution stability of substituted silylium and zirconocenium salts should be kinetic. However, other available WCAs perform better than $[B(C_6F_5)_4]^-$ and should therefore be tried in future in silylium and zirconocenium ion chemistry. We have shown that the FIA and the LA in combination with COSMO solvation calculations are valuable tools for determining the outcome of known reactions, that is, the solution stability of PCl_2^+ and OCX^+ salts (X = F, Cl). The calculated thermodynamics of these reactions mirrored the experiment and, by extrapolation to unknown reactions, this approach should be valuable for predictions of completely unknown transformations. The calculated data collected in Table 5 allow the assessment of relative thermodynamic stabilities of the respective anions in the presence of a desired target cation and to base a decision for a particular anion in preparative chemistry on several calculated thermodynamic criteria and not only on chemical intuition.

Computational Details

All calculations, except the G2 and CBS-Q calculations, were performed with the program TURBOMOLE.[55] The geometries were optimized at the (RI)-BP86,[56] B3LYP[56,57] and/or (RI)-MP2[58] level with the SV(P)[59] and TZVPP basis sets.[60] Frequency calculations[61] of hitherto unknown compounds were performed at the BP86/SV(P) level, and all species represent true minima without imaginary frequencies on the respective potential-energy surface. The G2[62] and CBS-Q[63] calculations were done with Gaussian 98.[64] Reaction energies are given at 0 K and do not include the zero-point energy; however, the error associated with this procedure is usually very small and has no influence on relative trends. For the G2 and CBS-Q calculations zero-point energies (MP2/TZVPP quality) and thermal corrections to the enthalpy at 298 K, as calculated with the program FreeH included with TURBOMOLE on the basis of the MP2/TZVPP geometries and frequencies, are included (see Supporting Information for a comment on this procedure). Approximate solvation energies (Ph–Cl solution with $\varepsilon_r = 5.69$ and 1,2-$F_2C_6H_4$ solution with $\varepsilon_r = 13.38$) were calculated with the COSMO model[65] at the BP86/SV(P) (DFT) level using the BP86/SV(P) geometries.

Appendix

Calculations of $[M(L)_n]^-$, $[M(L)_{n-1}]$, and $[FM(L)_{n-1}]^-$: Starting geometries for the optimization of most of the species were the orientations of available solid-state structures. For compounds not characterized by a solid-state or gas-phase structure, reasonable guesses for a starting geometry were obtained by force-field methods including molecular dynamics[66] and subsequent optimization of several isomers with BP86/SV(P). The nature of the stationary points obtained for the hitherto unknown species was examined by frequency calculations, and all compounds included in this paper are true minima with no negative eigenvalues of the Hessian matrix. Graphic representations of all compounds not shown in the Appendix are known from X-ray or electron diffraction and therefore not depicted. However, a figure of each such compound can be found in the Supporting Information.

Fluorometallate anions: This category has long been known, and the solid-state or gas-phase structures of almost all compounds included here are available, that is, those of BF_3 (ED), BF_4^- (XRD), MF_5 (ED), MF_6^- (M = P, As, Sb; XRD), $Sb_2F_{11}^-$ (XRD), Sb_3F_{15} (ED), $Sb_3F_{16}^-$ (XRD), Sb_4F_{20} (XRD), and $Sb_4F_{21}^-$ (XRD). The total energies and selected structural parameters of all calculated species are collected in Table 6. A comparison of the calculated and experimental parameters of the compounds in Table 6 shows good agreement for those species for which reliable experimental data are available. Usually, the calculated bond lengths are systematically overestimated by about 3–5 pm, as is well known for DFT calculations.[74] For some compounds, the agreement between experiment and calculation is worse, that is, deviations of up to 10 pm occur for $Sb_2F_{11}^-$. However, this is also attributed to shortcomings in the refinement of the crystal structures. Fluorinated compounds usually are heavily affected by librational motion that leads to bond lengths that appear to be shorter than the true distances, usually by 2–10 pm. Normally, the pa-

Table 6. Total energies and selected structural parameters of BF_3, BF_4^-, MF_5, MF_6^- (M = P, As, Sb), Sb_2F_{10}, $Sb_2F_{11}^-$, Sb_3F_{15}, $Sb_3F_{16}^-$, Sb_4F_{20}, and $Sb_4F_{21}^-$.

Species	Total energy [Hartree]	d(M−F$_{terminal}$) [pm]	Exptl d(M−F$_{terminal}$) [pm]	d(M−F$_{bridge}$) [pm]	Exptl d(M−F$_{bridge}$) [pm]
BF_3	−324.31769	132	130[67]	–	–
BF_4^-	−424.20099	142	137[67]	–	–
PF_5	−840.24920	ax: 161	ax: 158	–	–
		eq: 159	eq: 153[67]		
PF_6^-	−940.15393	165	158[68]	–	–
AsF_5	−2734.77740	ax: 174	ax: 171	–	–
		eq: 172	eq: 166[67]		
AsF_6^-	−2834.69432	177	168[68]	–	–
SbF_5	−504.34073	ax: 191	–	–	–
		eq: 193			
SbF_6^-	−604.28148	196	188[69]	–	–
Sb_2F_{10}	−1008.72990	191–192	–	214 (2x)	–
$Sb_2F_{11}^-$	−1108.68393	193–194	av: 185[69]	212	av: 202[69]
Sb_3F_{15}	−1513.10046	191	181[70]	211–212 (3×)	204–205[70]
$Sb_3F_{16}^-$ (*trans*)	−1613.06689	192–193	181–184[71]	218 (2×, outer)	197
				206 (2×, center)	210[71]
Sb_4F_{20}	−2017.47178	191	182[72]	211–212 (4×)	av: 203[72]
$Sb_4F_{21}^-$ (*trans*)	−2117.43906	192–193	184–185[73]	221 (2×, outer)	210
				203 (2×, middle)	198
				211 (2×, center)	201[73]

rameters of the crystal structures are not corrected for librational motion; therefore, the differences between experiment and calculations are larger by the additional amount of the missing librational correction.

The geometries of the Lewis acids Sb_nF_{5n} and the $[Sb_nF_{5n+1}]^-$ ions ($n = 3$, 4) were hitherto not calculated by quantum chemical methods and are shown in Figures 6 (neutral speciess) and 7 (anions). The data for Sb_2F_{10} and $[Sb_2F_{11}]^-$ are included for comparison.

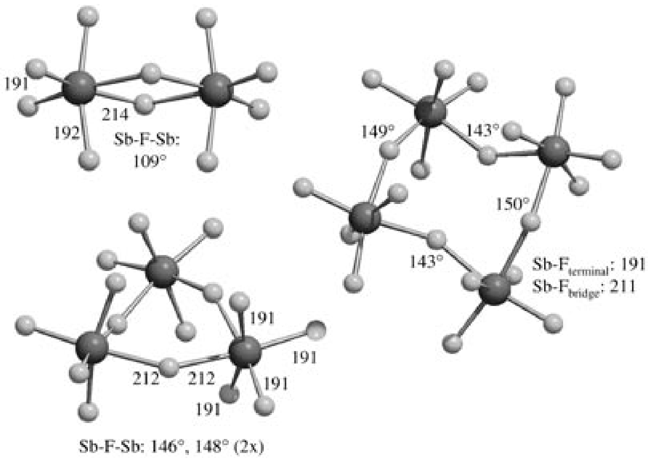

Figure 6. Calculated geometries of the Lewis acids Sb_nF_{5n} ($n = 2$, 3, 4).

No symmetry restraints were imposed on the molecules during optimization, but while Sb_3F_{15} and Sb_4F_{20} remained in C_1, the Sb_2F_{10} minimum shows D_{2h} symmetry. Note that the two sets of bridging Sb-F-Sb bond angles in solid Sb_4F_{20} (141 and 170°) are to a lesser extent also retained in the optimized calculated structure (143, 149/150°). Still the question remains whether or not the bond angle of 170° in the experimental structure is due to librational/packing effects.

Larger borate-based anions: The long-known parent compound of these anions is tetraphenylborate $[B(C_6H_5)_4]^-$, which becomes more stable and less coordinating upon replacing hydrogen atoms by fluorine atoms or CF_3 groups.[1b–d] Almost all geometries of the $[B(L)_4]^-$ type of anions and their corresponding Lewis acids $B(L)_3$ are available experimentally (i.e., L = Ph, C_6F_5, $C_6H_3(CF_3)_2$; for L = CF_3 only the anion). A recent addition to these borates are the diborane-based $[F_4C_6\{1,2\text{-}\{B(C_6F_5)_2\}_2\}F]^-$ and $[F_4C_6\{1,2\text{-}\{B(C_6F_5)_2\}_2\}OMe]^-$ ions, in which a univalent simple anion (F^- or OMe^-) is coordinated to two Lewis acidic boron centers. The total energies and basic structural parameters of these compounds are collected in Table 7; for drawings of the diborane Lewis acid $C_6F_4(B(C_6F_5)_2)_2$ and the respective anions with F^- and OMe^-, see Supporting Information. Calculated and experimental geometries are in excellent agreement and usually agree within 3–5 pm.

The $[F_4C_6\{1,2\text{-}\{B(C_6F_5)_2\}_2\}F]^-$ ion contains, to the best of our knowledge, the first example of a experimentally verified B-F-B bridge. However, no crystal structure data is available for the $[F_4C_6\{1,2\text{-}\{B(C_6F_5)_2\}_2\}F]^-$ ion, so that the optimized structure with a B-F-B bond angle of 116° provides the only available structural parameters for this important species. This B-F-B bridge is of great interest for understanding exchange processes of BF_3 with other BX_3 (X = Cl, Br, I) compounds. In contrast to the computational predictions for the $[X_3B{-}F{-}BX_3]^-$ ions (X = F, Cl),[82] the B-F-B bridge in $[F_4C_6\{1,2\text{-}\{B(C_6F_5)_2\}_2\}F]^-$ is not linear. Upon F^- complexation, the geometry requirements of the resulting five-membered C_2B_2F ring certainly account for this deviation from linearity. Note that the bridging B−F distance in $[F_4C_6\{1,2\text{-}\{B(C_6F_5)_2\}_2\}F]^-$ is about 19 pm or 13 % longer than that calculated for the terminal B−F bond in $[FB(C_6F_5)_3]^-$. This should be compared to the elongation of the terminal Sb−F bond in SbF_6^- upon complexation with SbF_5 and formation of the F-bridged $[Sb_2F_{11}]^-$ ion of 16 pm or 8 %. Therefore, the bridging fluoride in $[F_4C_6\{1,2\text{-}\{B(C_6F_5)_2\}_2\}F]^-$ is more labile that that in $[Sb_2F_{11}]^-$.

Aluminate-based anions: The perfluoro-*tert*-butoxyaluminates are a recent addition to the WCAs.[39,40,83–85] The structures of $[Al(OR)_4]^-$[39] and centrosymmetric $[(RO)_3AlFAl(OR)_3]^-$ are known (R = $C(CF_3)_3$).[31] Neither $[FAl(OR)_3]^-$ nor $Al(OR)_3$ and $Al_2(OR)_5F$ are known experimentally. However, the $Al(OR)_3{\cdot}THF$ adduct has been prepared,[86] and previously $Al(OR)_3$ was also optimized by DFT theory.[39] The current optimized structure including the two short Al−F contacts at 212 and 214 pm is in good agreement with that published. Two structures of the parent Lewis acid of $[(RO)_3AlFAl(OR)_3]^-$, that is, $Al_2(OR)_5F$, were found: the O- and F-bridged isomer I was preoptimized with molecular mechanics and subsequently fully optimized by DFT, while isomer II was obtained

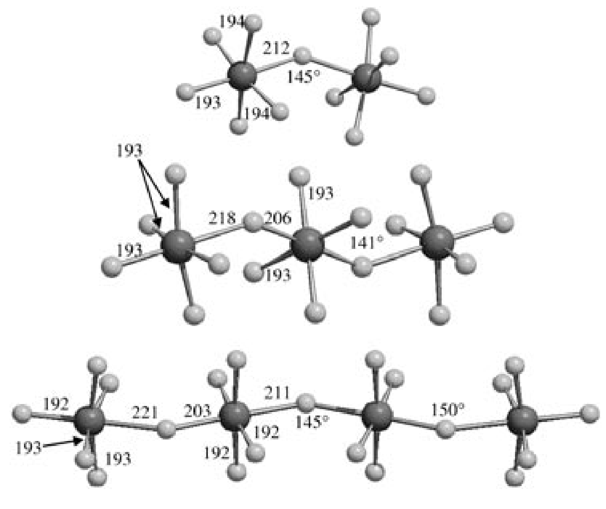

Figure 7. Calculated geometries of the anions $[Sb_nF_{5n+1}]^-$ ($n = 2$, 3, 4).

Table 7. Total energies and selected structural parameters of $B(C_6H_5)_3$, $[FB(C_6H_5)_3]^-$, $[B(C_6H_5)_4]^-$, $B(C_6F_5)_3$, $[FB(C_6F_5)_3]^-$, $[B(C_6F_5)_4]^-$, $B[C_6H_3(CF_3)_2]_3$, $[FB\{C_6H_3(CF_3)_2\}_3]^-$, $[B\{C_6H_3(CF_3)_2\}_4]^-$, $F_4C_6\{1,2\text{-}[B(C_6F_5)_2]_2\}$, $[F_4C_6\{1,2\text{-}[B(C_6F_5)_2]_2\}F]^-$, $[F_4C_6\{1,2\text{-}[B(C_6F_5)_2]_2\}OMe]^-$, $B(CF_3)_3$, $[FB(CF_3)_3]^-$, and $[B(CF_3)_4]^-$ (E = F, O, C).

Species	Total energy [Hartree]	d(B−E) [pm]	Exptl d(B−E) [pm]
$B(C_6H_5)_3$	−719.29596	B−C: 158	B−C: 156[68]
$[FB(C_6H_5)_3]^-$	−819.18095	B−C: 165 B−F: 146	–
$[B(C_6H_5)_4]^-$	−950.83873	B−C: 166	B−C: 164[68]
$B(C_6F_5)_3$	−2206.75303	B−C: 157	–
$[FB(C_6F_5)_3]^-$	−2306.67670	B−C: 167 B−F: 143	B−F: 143 B−C: 165[75]
$[B(C_6F_5)_4]^-$	−2934.16731	B−C: 167	B−C: 165[76]
$B\{C_6H_3(CF_3)_2\}_3$	−2740.16531	B−C: 157	B−C: 165
$[FB\{C_6H_3(CF_3)_2\}_3]^-$	−2840.09918	B−C: 165 B−F: 145	–
$[B\{C_6H_3(CF_3)_2\}_4]^-$	−3645.39000	B−C: 166	B−C: 163–164[77]
$F_4C_6[1,2\text{-}\{(B(C_6F_5)_2\}_2]$	−3586.44640	B−C: 157–158	B−C: 157[78]
$[F_4C_6\{1,2\text{-}[B(C_6F_5)_2]_2\}F]^-$	−3686.39740	B−C: 161–164 B−F: 162–163	–
$[F_4C_6\{1,2\text{-}[B(C_6F_5)_2]_2\}OMe]^-$	−3701.66354	B−C: 162–166 B−O: 159	B−C: 158–161 B−O: 155–157[79]
$B(CF_3)_3$	−1037.00999	B−C: 161	–
$[FB(CF_3)_3]^-$	−1136.97489	B−C: 165 B−F: 143	B−F: 141 B−C: 163[80]
$[B(CF_3)_4]^-$	−1374.57139	B−C: 165	B−C: 163[81]

Table 8. Total energies and selected structural parameters of $Al(OR)_3$, $[FAl(OR)_3]^-$, $[Al(OR)_4]^-$, two isomers of $Al_2(OR)_5F$, and $[(RO)_3AlFAl(OR)_3]^-$ ($R = C(CF_3)_3$).

Species	Total energy [Hartree]	d(Al−O) [pm]	d(Al−F) [pm]	Exptl d(Al−O/F) [pm]
$Al(OR)_3$	−3618.91742	171, 176 (2×)	212, 214	–
$[FAl(OR)_3]^-$	−3718.87659	177, 178 (2×)	169	–
$[Al(OR)_4]^-$	−4744.54880	176	–	O: 173[39]
$Al_2(OR)_5F$ (I)	−6212.21353	170–173	182, 184	–
$(RO)_3AlFAl(OR)_2$ (II)	−6212.18358	170–175	174, 191, 195	–
$[(RO)_3AlFAl(OR)_3]^-$	−7337.85243	174–175	183	O: 169, F: 177[31]

by simply deleting one OR ligand of the structure of the $[(RO)_3AlF\text{-}Al(OR)_3]^-$ ion and optimizing the resulting neutral species. Both species are true minima with no imaginary frequencies. Isomer I may be viewed as the thermodynamic product of OR abstraction from $[(RO)_3AlF\text{-}Al(OR)_3]^-$, and isomer II as the kinetic (approximately vertical) product. For the $(RO)_3AlFAl(OR)_2$ Lewis acid (isomer II), the crystal structure of one adduct with OPI_3, that is, $(RO)_3AlFAl(OR)_2{\cdot}OPI_3$, is known.[86] The total energies and basic structural parameters of the aluminum compounds are collected in Table 8.

Comparison to available experimental structures shows that the calculations reproduce the geometries within the typical 3–6 pm overestimation of the bond lengths. Two of the optimized Lewis acid geometries, that is, $Al(OR)_3$ and $(RO)_3AlFAl(OR)_2$ (isomer II), are remarkable in that they contain Al-F-C bridges to intramolecularly aluminum coordinated CF_3 groups at $d(Al{-}F) = 195\text{–}214$ pm. Upon coordination, the respective C−F bonds are elongated from about 133 to 143–144 pm ($Al(OR)_3$) or even 151 pm ($(RO)_3AlFAl(OR)_2$). This highlights the strongly Lewis acidic character of the formally tricoordinate aluminum centers in $Al(OR)_3$ and $(RO)_3AlFAl(OR)_2$ (isomer II). Since a considerable atomic rearrangement from the structure of isomer II to isomer I must occur, the $(RO)_3AlFAl(OR)_2$ (isomer II) structure is likely to be initially formed upon decomposition of the $[(RO)_3Al\text{-}FAl(OR)_3]^-$ ion for kinetic reasons. Therefore, we consider isomer II as being important for the stability of the anion, as in Table 5. The LA, PD, and CuD values for the formation of isomer I in Table 5 are given in parentheses. The optimized DFT structures of the Lewis acids are shown in Figures 8 ($Al(OR)_3$) and 9 (two isomers of $Al_2(OR)_5F$).

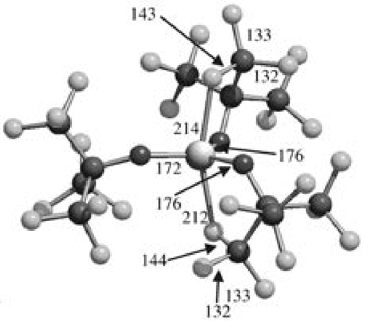

Figure 8. Optimized DFT structure of $Al(OR)_3$.

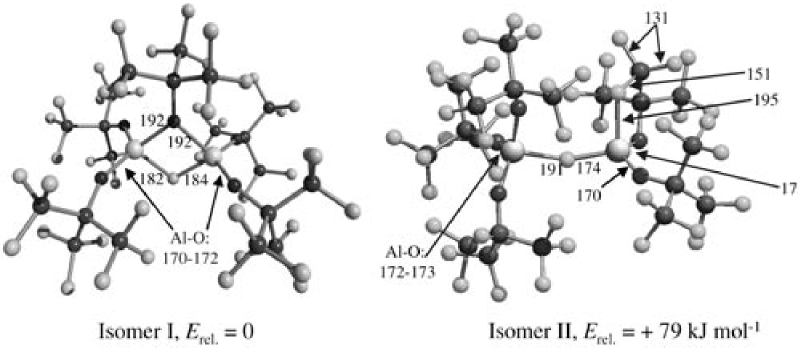

Isomer I, $E_{rel.} = 0$

Isomer II, $E_{rel.} = +79\ kJ\ mol^{-1}$

Figure 9. Optimized DFT structures of two isomers of $Al_2(OR)_5F$.

Teflate-based anions: This class of anions contains the larger univalent $OTeF_5$ group as a substitute for the fluoride ion in the fluorometallate anions. The solid-state structures of the compounds $B(OTeF_5)_3$, $[B(OTeF_5)_4]^-$, $[FAs(OTeF_5)_5]^-$ and $[M(OTeF_5)_6]^-$ (M = As, Sb) are known; only the structures of $M(OTeF_5)_5$, $[F{-}B(OTeF_5)_3]^-$, and $[F{-}Sb(OTeF_5)_5]^-$ are unknown experimentally. The total energies and structural parameters of all teflate-based compounds are collected in Table 9; a drawing of the optimized $M(OTeF_5)_5$ structure is shown in Figure 10.

Comparison of the calculated with available experimental parameters shows that the M−O and O−Te bond lengths in the calculated structures are 8–10 pm longer than those in the experimental structures. Similarly, the calculated M-O-Te bond angles are 10 to 20° more acute than the experimental values. Both observations are consistent with the notion that the experimental values may strongly be affected by libration. Moreover, the light oxygen atom is always located

Table 9. Total energies and selected structural parameters of $B(OTeF_5)_3$, $[FB(OTeF_5)_3]^-$, $[B(OTeF_5)_4]^-$, $M(OTeF_5)_5$, $[FM(OTeF_5)_5]^-$, and $[M(OTeF_5)_6]^-$ (M = As, Sb).

Species	Total energy [Hartree]	d(E–O/F) [pm]	d(Te–O) [pm]	Exptl d(E–O/F) [pm]
$B(OTeF_5)_3$	−1771.19343	B–O: 138	198	B–O: 136 Te–O: 187
$[FB(OTeF_5)_3]^-$	−1871.15753	B–O: 150 B–F: 137	193	–
$[B(OTeF_5)_4]^-$	−2353.45910	B–O: 148	194	B–O: 146–147 Te–O: 184–186[87]
$As(OTeF_5)_5$	−5146.23686	As–O_{eq}: 178 As–O_{ax}: 182–183	202	–
$[FAs(OTeF_5)_5]^-$	−5246.21734	As–F: 175 As–O_{eq}: 186 As–O_{ax}: 187	196	As–F: 173 As–O_{av}: 181 Te–O_{av}: 185[88]
$[As(OTeF_5)_6]^-$	−5728.50888	As–O: 186–186	196	As–O_{av}: 181 Te–O_{av}: 185[88]
$Sb(OTeF_5)_5$	−2915.82156	Sb–O_{eq}: 198–199 Sb–O_{ax}: 201	199	–
$[FSb(OTeF_5)_5]^-$	−3015.81738	Sb–F: 193 Sb–O_{eq}: 204 Sb–O_{ax}: 205	194	–
$[Sb(OTeF_5)_6]^-$	−3498.11271	Sb–O: 203–204	195	Sb–O_{av}: 195 Te–O_{av}: 184[89]

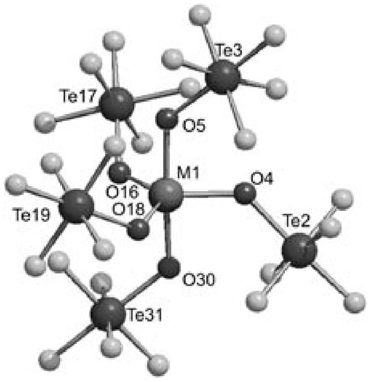

Figure 10. Optimized BP86/SV(P) structure of $M(OTeF_5)_5$. Selected bond lengths in pm: As1–O4: 178, As1–O18: 178, As1–O16: 178, As1–O5: 182, As1–O30: 183, Sb1–O4: 198, Sb1–O18: 199, Sb1–O16: 199, Sb1–O5: 201, Sb1–O30: 210; $d(\text{Te–O})_{ave}$: 202 (M = As), 199 (M = Sb); $d(\text{Te–F})_{ave}$: 191 (M = As,Sb); $(\text{As-O-Te})_{ave}$: 133°; $(\text{Sb-O-Te})_{ave}$: 130°.

between two very heavy atoms (M and Te), further decreasing the accuracy of the determination of the position of the oxygen atom in the crystal structure. Libration would increase the M-O-Te bond angle and decrease the M–O and Te–O bond lengths. Therefore, we suggest that the true M–O/Te–O bond lengths and M-O-Te bond angles should be expected somewhere between the calculated and the librationally uncorrected experimental values. From experimental work it is known[90] that $As(OTeF_5)_5$ is a stable compound, while the antimony analogue $Sb(OTeF_5)_5$ decomposes easily and cannot be used as a reagent. See Supporting Information for a comment.

Acknowledgement

We thank Prof. H. Schnöckel and Prof. J. Passmore for valuable discussions and advice. Financial support from the German science foundation DFG, a Heisenberg-fellowship (I.K.), and financial support from the Fonds der Chemischen Industrie are gratefully acknowledged.

---

[1] Reviews: a) C. Reed, *Acc. Chem. Res.* **1998**, *31*, 133; b) S. H. Strauss, *Chem. Rev.* **1993**, *93*, 927; c) E. Y.-X. Chen, T. J. Marks, *Chem. Rev.* **2000**, *100*, 1391; d) I. Krossing, I. Raabe, *Angew. Chem.* **2004**, *116*, 2216; *Angew. Chem. Int. Ed.* **2004**, *43*, 2066.

[2] a) J. Zhou, S. J. Lancaster, D. A. Walker, S. Beck, M. Thornton-Pett, M. Bochmann, *J. Am. Chem. Soc.* **2001**, *123*, 223; b) R. E. LaPointe, G. R. Roof, K. A. Abboud, J. Klosin, *J. Am. Chem. Soc.* **2000**, *122*, 9560; c) V. C. Williams, G. J. Irvine, W. E. Piers, Z. Li, S. Collins, W. Clegg, M. R. J. Elsegood, T. B. Marder, *Organometallics* **2000**, *19*, 1619; d) E. Y. X. Chen, K. Abboud, *Organometallics* **2000**, *19*, 5541.

[3] a) K. Fujiki, S. Ikeda, H. Kobayashi, A. Mori, A. Nagira, J. Nie, T. Sonoda, Y. Yagupolskii, *Chem. Lett.* **2000**, 66; b) T. J. Barbarich, S. M. Miller, O. P. Anderson, S. H. Strauss, *J. Mol. Catal. A: Chem.* **1998**, *128*, 289.

[4] N. J. Patmore, C. Hague, J. H. Cotgreave, M. F. Mahon, C. G. Frost, A. S. Weller, *Chem. Eur. J.* **2002**, *8*, 2088.

[5] K. Fujiki, S. Ikeda, H. Kobayashi, A. Mori, A. Nagira, J. Nie, T. Sonoda, Y. Yagupolskii, *Chem. Lett.* **2000**, 66.

[6] a) S. D. Ittel, L. K. Johnson, M. Brookhart, *Chem. Rev.* **2000**, *100*, 1169; b) G. J. P. Britovsek, V. C. Gibson, D. F. Wass, *Angew. Chem.* **1999**, *111*, 448; *Angew. Chem. Int. Ed.* **1999**, *38*, 429; c) S. Mecking, *Coord. Chem. Rev.* **2000**, *203*, 305.

[7] a) H. H. Brintzinger, D. Fischer, R. Mülhaupt, B. Rieger, R. Waymouth, *Angew. Chem.* **1995**, *107*, 1255; *Angew. Chem. Int. Ed.* **1995**, *34*, 1143; b) W. E. Piers, *Chem. Eur. J.* **1998**, *4*, 13; c) C. Zuccaccia, N. G. Stahl, A. Macchioni, M.-C. Chen, J. A. Roberts, T. J. Marks, *J. Am. Chem. Soc.* **2004**, *126*, 1448; d) M.-C. Chen, J. A. Roberts, T. J. Marks, *Organometallics* **2004**, *23*, 932; e) M.-C. Chen, J. A. Roberts, T. J. Marks, *J. Am. Chem. Soc.* **2004**, *126*, 4605.

[8] For recent reviews, see a) P. Wasserscheid, W. Keim, *Angew. Chem.* **2000**, *112*, 3926; *Angew. Chem. Int. Ed.* **2000**, *39*, 3772; b) J. D. Holbrey, *Clean Prod. Processes* **1999**, *1*, 2071; c) T. Welton, *Chem. Rev.* **1999**, *99*, 2071.

[9] A. Bösmann, G. Francio, E. Janssen, W. Leitner, P. Wasserscheid, *Angew. Chem.* **2001**, *113*, 2769; *Angew. Chem. Int. Ed.* **2001**, *40*, 2697.

[10] a) R. J. LeSuer, W. E. Geiger, *Angew. Chem.* **2000**, *112*, 254; *Angew. Chem. Int. Ed.* **2000**, *39*, 248; b) F. Barriere, N. Camire, W. E. Geiger, U. T. Mueller-Westerhoff, R. Sanders, *J. Am. Chem. Soc.* **2002**, *124*, 7262; c) N. Camire, A. Nafady, W. E. Geiger, *J. Am. Chem. Soc.* **2002**, *124*, 7260; d) N. Camire, U. T. Mueller-Westerhoff, W. E. Geiger, *J. Organomet. Chem.* **2001**, *637–639*, 823.

[11] a) P. G. Gassman, P. A. Deck, *Organometallics* **1994**, *13*, 1934; b) M. G. Hill, W. M. Lamanna, K. R. Mann, *Inorg. Chem.* **1991**, *30*, 4687; c) P. G. Gassman, J. R. Sowa Jr., M. G. Hill, K. R. Mann, *Organometallics* **1995**, *14*, 4879.

[12] L. Pospisil, B. T. King, J. Michl, *Electrochim. Acta* **1998**, *44*, 103.

[13] J. V. Crivello in *Radiation Curing in Polymer Science and Technology, Vol. 2* (Eds. J. P. Fouassier, J. F. Rabek), Chapmann & Hall, London, **1993**, 435.

[14] F. Castellanos, J. P. Fouassier, C. Priou, J. Cavezzan, *J. Appl. Polym. Sci.* **1996**, *60*, 705.

[15] a) K. Ren, A. Mejiritski, J. H. Malpert, O. Grinevich, H. Gu, D. C. Neckers, *Tetrahedron Lett.* **2000**, *41*, 8669; b) H. Li, K. Ren, W. Zhang, J. H. Malpert, D. C. Neckers, *Macromolecules* **2001**, *34*, 4161; c) H. Gu, K. Ren, A. Mejiritski, O. Grinevich, J. H. Malpert, D. C. Neckers, *J. Org. Chem.* **2001**, *66*, 4161.

[16] K. Ren, J. H. Malpert, H. Li, H. Gu, D. C. Neckers, *Macromolecules* **2002**, *35*, 1632.

[17] a) F. Kita, H. Sakata, A. Kawakami, H. Kamizori, T. Sonoda, H. Nagashima, N. V. Pavlenko, Y. Yagupolskii, *J. Power Sources* **2001**, *97–98*, 581; b) L. M. Yagupolski, L. Yu, J. Yagupolski, *J. Fluorine Chem.* **1995**, *72*, 225; c) N. Ignat'tev, P. Sartori, *J. Fluorine Chem.* **2001**, *101*, 203.

[18] F. Kita, H. Sakata, S. Sinomoto, A. Kawakami, H. Kamizori, T. Sonoda, H. Nagashima, J. Nie, N. V. Pavlenko, Y. Yagupolskii, *J. Power Sources* **2000**, *90*, 27.

[19] W. Xu, C. A. Austen, *Electrochem. Solid-State Lett.* **2000**, *3*, 366.

[20] S. Seidel, K. Seppelt, *Science* **2000**, *290*, 117.

[21] T. Drews, K. Seppelt, *Angew. Chem.* **1997**, *109*, 264; *Angew. Chem. Int. Ed. Engl.* **1997**, *36*, 273.

[22] C. A. Reed, K.-C. Chan, R. D. Bolskar, L. J. Mueller, *Science* **2000**, *289*, 101.

[23] K. C. Chan, C. A. Reed, D. W. Elliott, L. J. Mueller, F. Tham, L. Lin, J. B. Lambert, *Science* **2002**, *297*, 825.

[24] P. K. Hurlburt, J. J. Rack, J. S. Luck, S. F. Dec, J. D. Webb, O. P. Anderson, S. H. Strauss, *J. Am. Chem. Soc.* **1994**, *116*, 10003.

[25] A. Vij, W. W. Wilson, V. Vij, F. S. Tham, J. A. Sheehy, K. O. Christe, *J. Am. Chem. Soc.* **2001**, *123*, 6308.

[26] B. von Ahsen, M. Berkei, G. Henkel, H. Willner, F. Aubke, *J. Am. Chem. Soc.* **2002**, *124*, 8371.

[27] a) I. Krossing, *J. Am. Chem. Soc.* **2001**, *123*, 4603–4604; b) I. Krossing, L. van Wüllen, *Chem. Eur. J.* **2002**, *8*, 700.

[28] T. S. Cameron, A. Decken, I. Dionne, M. Fang, I. Krossing, J. Passmore, *Chem. Eur. J.* **2002**, *8*, 3386.

[29] A. Adolf, M. Gonsior, I. Krossing, *J. Am. Chem. Soc.* **2002**, *124*, 7111.

[30] A. Reisinger, I. Krossing, *Angew. Chem.* **2003**, *115*, 5903; *Angew. Chem. Int. Ed.* **2003**, *42*, 5725.

[31] a) I. Krossing, *J. Chem. Soc. Dalton Trans.* **2002**, 500; b) I. Krossing, I. Raabe, *Angew. Chem.* **2001**, *113*, 4544; *Angew. Chem. Int. Ed.* **2001**, *40*, 4406.

[32] A. Bihlmeier, I. Krossing, I. Raabe, N. Trapp, *Angew. Chem.* **2003**, *115*, 1569; *Angew. Chem. Int. Ed.* **2003**, *42*, 1531.

[33] H. P. A. Mercier, M. D. Moran, G. J. Schrobilgen, C. Steinberg, R. J. Suontamo, *J. Am. Chem. Soc.* **2004**, *126*, 5533.

[34] See the most recent update of this scale: C. A. Reed, D. Stasko, *J. Am. Chem. Soc.* **2002**, *124*, 1148.

[35] C. A. Reed, presented at the ACS national meeting in New Orleans in March **2003**.

[36] a) T. E. Mallouk, G. L. Rosenthal, G. Muller, R. Brusasco, N. Bartlett, *Inorg. Chem.* **1984**, *23*, 3167; b) H. K. Roobottom, H. D. B. Jenkins, J. Passmore, L. Glasser, *Inorg. Chem.* **1999**, *38*, 3609; H. D. B. Jenkins, H. K. Roobottom, J. Passmore, *Inorg. Chem.* **2003**, *42*, 2886.

[37] K. O. Christe, D. A. Dixon, D. McLemore, W. W. Wilson, J. Sheehy, J. A. Bootz, *J. Fluorine Chem.* **2000**, *101*, 151.

[38] a) T. S. Cameron, R. J. Deeth, I. Dionne, H. Du, H. D. B. Jenkins, I. Krossing, J. Passmore, H. K. Roobottom, *Inorg. Chem.* **2000**, *39*, 5614; b) I.-C. Hwang, K. Seppelt, *Angew. Chem.* **2001**, *113*, 3803; *Angew. Chem. Int. Ed.* **2001**, *40*, 3690; c) S. Brownridge, H. D. B. Jenkins, I. Krossing, J. Passmore, H. K. Roobottom, *Coord. Chem. Rev.* **2000**, *197*, 397.

[39] I. Krossing, *Chem. Eur. J.* **2001**, *7*, 490.

[40] M. Gonsior, I. Krossing, N. Mitzel, *Z. Anorg. Allg. Chem.* **2002**, *628*, 1821.

[41] M. Finze, M. Zähres, H. Willner, *Inorg. Chem.* **2004**, *43*, 490.

[42] Standard enthalpies of formation were taken from the website of the National Institute of Standards and Technology at: http://webbook.nist.gov/chemistry/.

[43] I. A. Koppel, P. Burk, I. Koppel, I. Leito, T. Sonoda, M. Mishima, *J. Am. Chem. Soc.* **2000**, *122*, 5114.

[44] For reviews, see a) J. B. Lambert, L. Kania, S. Zhang, *Chem. Rev.* **1995**, *95*, 1191; b) C. A. Reed, *Acc. Chem. Res.* **1998**, *31*, 325.

[45] D. M. Van Seggan, P. K. Hurtburt, M. D. Noirot, O. P. Anderson, S. H. Strauss, *Inorg. Chem.* **1992**, *31*, 1423.

[46] W. V. Konze, B. L. Scott, G. J. Kubas, *Chem. Commun.* **1999**, 1807.

[47] D. A. Walker, T. J. Woodman, D. L. Hughes, M. L. Bochmann, *Organometallics* **2001**, *20*, 3772.

[48] a) P. Biagini, G. Luigli, L. Abis, P. Andeussi, US 5602269, **1997** (Enichem); b) M. Bochmann, M. J. Sarsfield, *Organometallics* **1998**, *17*, 5908.

[49] A. Bihlmeier, M. Gonsior, I. Krossing, I. Raabe, N. Trapp, *Chem. Eur. J.* **2004**, *10*, in press.

[50] Equation (13) is best calculated via Equation (16) (here MP2/TZVPP) and Equation (2). The reaction energy of Equation (2) can be taken from Table 4.

$$\mathrm{PCl_2^+ + [(RO)AlF_3]^-} \xrightarrow{\Delta_rU\,=\,-468} \mathrm{RO\text{-}PCl_2 + AlF_3} \qquad (16)$$

$$\mathrm{RO^- + AlF_3} \xrightarrow{\Delta_rU\,=\,-321} \mathrm{[(RO)AlF_3]^-} \qquad [\text{Eq. (2)/Table 8}]$$

$$\mathrm{PCl_2^+ + OR^-} \xrightarrow{\Delta_rU\,=\,-789} \mathrm{RO\text{-}PCl_2} \qquad (13)$$

[51] The isodesmic reaction in Equation (17) was calculated by MP2/TZVPP, and thereto the experimentally known enthalpy of reaction given in Equation (18) of $+209\ \mathrm{kJ\,mol^{-1}}$ was added:

$$\mathrm{2\,F_2CO} \xrightarrow{\Delta_rU\,=\,867\ \mathrm{kJ\,mol^{-1}}} \mathrm{FCO^+ + OCF_3^-} \qquad (17)$$

$$\mathrm{OCF_3^-} \xrightarrow{\Delta_rH\,=\,209\ \mathrm{kJ\,mol^{-1}}} \mathrm{F^- + F_2CO} \qquad (18)$$

$$\mathrm{F_2CO} \xrightarrow{\Delta_rU\,=\,1076\ \mathrm{kJ\,mol^{-1}}} \mathrm{FCO^+ + F^-} \qquad (15)$$

[52] One may argue that 1,2-$F_2C_6H_4$ is not a suitable solvent for this reaction, but liquid SO_2, which is a likely solvent for Equation (14), has a very similar polarity ($\varepsilon_r = 14$ at 20 °C).

[53] K. O. Christe, B. Hoge, J. A. Boatz, G. K. S. Prakash, G. A. Olah, J. A. Sheehy, *Inorg. Chem.* **1999**, *38*, 3132–3142.

[54] See also E. Bernhardt, H. Willner, F. Aubke, *Angew. Chem.* **1999**, *111*, 830; *Angew. Chem. Int. Ed.* **1999**, *38*, 823.

[55] R. Ahlrichs, M. Bär, M. Häser, H. Horn, C. Kölmel, *Chem. Phys. Lett.* **1989**, *162*, 165.

[56] a) J. C. Slater, *Phys. Rev.* **1951**, *81*, 385; b) S. H. Vosko, L. Wilk, M. Nusair, *Can. J. Phys.* **1980**, *58*, 1200; c) A. D. Becke, *Phys. Rev. A* **1988**, *38*, 3098; e) J. P. Perdew, *Phys. Rev. B* **1986** *33*, 8822.

[57] a) C. Lee, W. Yang, R. G. Parr, *Phys. Rev. B* **1988**, *37*, 785; b) A. D. Becke, *J. Chem. Phys.* **1993**, *98*, 5648.

[58] a) F. Weigend, M. Häser, *Theor. Chim. Acta* **1997**, *97*, 331; b) F. Weigend, M. Häser, H. Patzelt, R. Ahlrichs, *Chem. Phys. Lett.* **1998**, *294*, 143.

[59] K. Eichkorn, O. Treutler, H. Oehm, M. Häser, R. Ahlrichs, *Chem. Phys. Lett.* **1995**, *242*, 652.

[60] A. Schäfer, C. Huber, R. Ahlrichs, *J. Chem. Phys.* **1994**, *100*, 346.

[61] P. Deglmann, F. Furche, R. Ahlrichs, *Chem. Phys. Lett.* **2002**, *362*, 511.

[62] L. A. Curtiss, K. Raghavachari, G. W. Trucks, J. A. Pople, *J. Chem. Phys.* **1991**, *94*, 7221.

[63] a) G. A. Petersson, T. G. Tensfeldt, J. A. Montgomery Jr., *J. Chem. Phys.* **1991**, *94*, 6091; b) J. W. Ochterski, G. A. Petersson, J. A. Montgomery Jr., *J. Chem. Phys.* **1996**, *104*, 2598.

[64] Gaussian 98 (Revision A.11), M. J. Frisch, G. W. Trucks, H. B. Schlegel, G. E. Scuseria, M. A. Robb, J. R. Cheeseman, V. G. Zakrzewski, J. A. Montgomery, Jr., R. E. Stratmann, J. C. Burant, S. Dapprich, J. M. Millam, A. D. Daniels, K. N. Kudin, M. C. Strain, O. Farkas, J. Tomasi, V. Barone, M. Cossi, R. Cammi, B. Mennucci, C. Pomelli, C. Adamo, S. Clifford, J. Ochterski, G. A. Petersson, P. Y. Ayala, Q. Cui, K. Morokuma, D. K. Malick, A. D. Rabuck, K. Raghavachari, J. B. Foresman, J. Cioslowski, J. V. Ortiz, B. B. Stefanov, G. Liu, A. Liashenko, P. Piskorz, I. Komaromi, R. Gomperts, R. L. Martin, D. J. Fox, T. Keith, M. A. Al-Laham, C. Y. Peng, A. Nanayakkara, C. Gonzalez, M. Challacombe, P. M. W. Gill, B. G. Johnson, W. Chen, M. W. Wong, J. L. Andres, M. Head-Gordon, E. S. Replogle, J. A. Pople, Gaussian, Inc., Pittsburgh, PA, **2001**.

[65] A. Klamt, G. Schürmann, *J. Chem. Soc. Perkin Trans. 2* **1993**, *2*, 799.

[66] Done with the program CHEM 3D from CambridgeSoft.

[67] Holleman-Wiberg, *Lehrbuch der Anorganischen Chemie*, 101st ed., de Gruyter, Berlin, New York, **1995**.

[68] *CRC Handbook of Chemistry and Physics*, 80th Ed. (Ed.: D. R. Lide), CRC, Boca Raton, **2000**.

[69] A. Vij, F. S. Tham, V. Vij, W. W. Wilson, K. O. Christe, *Inorg. Chem.* **2002**, *41*, 6397.

[70] J. Brunvoll, A. A. Ishchenko, I. N. Myakshin, G. V. Romanov, V. P. Spiridonov, T. G. Strand, V. F. Sukhoverkhov, *Acta Chem. Scand. Ser. A* **1980**, *34*, 733.

[71] A. J. Edwards, G. R. Jones, *J. Chem. Soc. A* **1973**, 2318.

[72] A. J. Edwards, P. Taylor, *J. Chem. Soc. Chem. Commun.* **1971**, 1376.
[73] T. Drews, K. Seppelt, *Angew. Chem.* **1997**, *109*, 264; *Angew. Chem. Int. Ed. Engl.* **1997**, *36*, 273.
[74] W. Koch, M. C. Holthausen, *A Chemists Guide to DFT*, Wiley-VCH, Weinheim, **2000**.
[75] R. Taube, S. Wache, J. Sieler, *J. Organomet. Chem.* **1993**, *459*, 335.
[76] E. B. Tjaden, D. C. Swenson, R. F. Jordan, J. L. Petersen, *Organometallics* **1995**, *14*, 371.
[77] J. L. Priego, L. H. Doerrer, L. H. Rees, M. H. L. Green, *Chem. Commun.* **2000**, 779.
[78] V. C. Williams, W. E. Piers, W. Clegg, S. Collins, T. B. Marder, *J. Am. Chem. Soc.* **1999**, *121*, 3244.
[79] a) L. D. Henderson, W. E. Piers, G. J. Irvine, R. McDonald, *Organometallics* **2002**, *21*, 340; V. C. Williams, G. J. Irvine, W. E. Piers, Z. Li, S. Collins, W. Clegg, M. R. J. Elsegood, T. B. Marder, *Organometallics* **2000**, *19*, 1619.
[80] E. Bernhardt, M. Finze, C. W. Lehmann, F. Aubke, *Angew. Chem.* **2003**, *115*, 2123; *Angew. Chem. Int. Ed.* **2003**, *42*, 2077.
[81] E. Bernhardt, G. Henkel, H. Willner, G. Pawelke, H. Bürger, *Chem. Eur. J.* **2001**, *7*, 4696.
[82] S. D. Williams, W. Harper, G. Mamantov, L. J. Tortorelli, G. Shankle, *J. Comput. Chem.* **1996**, *17*, 1696.
[83] a) T. J. Barbarich, S. T. Handy, S. M. Miller, O. P. Anderson, P. A. Grieco, S. H. Strauss, *Organometallics* **1996**, *15*, 3776; b) T. J. Barbarich, S. M. Miller, O. P. Anderson, S. H. Strauss, *J. Mol. Catal. A: Chem.* **1998**, *128*, 289; c) S. M. Ivanova, B. G. Nolan, Y. Kobayashi, S. M. Miller, O. P. Anderson, S. H. Strauss, *Chem. Eur. J.* **2001**, *7*, 503.
[84] S. H. Strauss, B. G. Nolan, B. P. Fauber, WO 00/53611, **2000**.
[85] I. Krossing, H. Brands, R. Feuerhake, S. Koenig, *J. Fluorine Chem.* **2001**, *112*, 83.
[86] M. Gonsior, I. Krossing, unpublished.
[87] D. M. Van Seggan, P. K. Hurtburt, M. D. Noirot, O. P. Anderson, S. H. Strauss, *Inorg. Chem.* **1992**, *31*, 1423.
[88] M. Gerken, P. Kolb, A. Wegner, H. P. A. Mercier, H. Borrmann, D. A. Dixon, G. J. Schrobilgen, *Inorg. Chem.* **2000**, *39*, 2813.
[89] W. J. Casteel Jr., P. Kolb, N. LeBlond, H. P. A. Mercier, G. J. Schrobilgen, *Inorg. Chem.* **1996**, *35*, 929.
[90] H. P. A. Mercier, J. C. P. Saunders, G. J. Schrobilgen, *J. Am. Chem. Soc.* **1994**, *116*, 2921.

Received: January 26, 2004
Revised: May 18, 2004